Connecting deterministic and numerical methods to better estimate the probability of flooding for clay dikes

P.H.E. Voorn

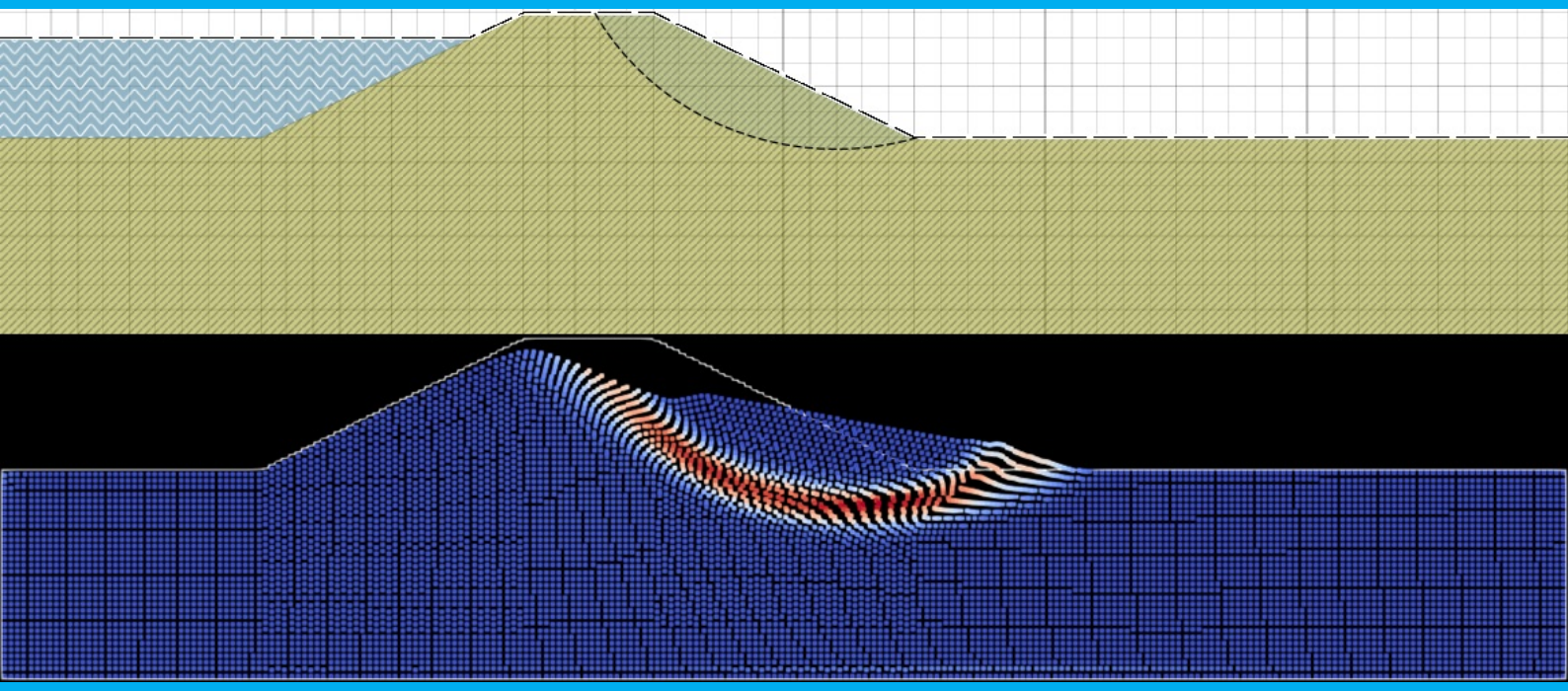

TU Delft

Connecting deterministic and numerical methods to better estimate the probability of flooding for clay dikes

by

P.H.E. Voorn

to obtain the degree of Master of Science
at the Delft University of Technology,
to be defended publicly on July 1st, 2021 at 09.15

Student number:	428726	
Project duration:	September 1, 2020 – July 1, 2021	
Thesis committee:	Dr. P. J. Vardon,	TU Delft, supervisor
	Dr. ir. T. Schweckendiek,	TU Delft
	Ir. M. G. Van der Krogt,	TU Delft
	Ir. G. Remmerswaal,	TU Delft

An electronic version of this thesis is available at `http://repository.tudelft.nl/`.

TU Delft

Preface

Large projects like these are never done alone and this thesis is no exception. Although the pandemic made it difficult to physically meet people, I have felt support from all sides throughout the creation of this work.

First I would like to thank my committee. Although we have not met yet, I always felt that you were all engaged in the project. I would like to thank Phil Vardon and Timo Schweckendiek for their keen analyses, steering me in the right direction where that was needed. I also would like to thank Mark Van der Krogt for his time and his insightful comments, which made sure every aspect was covered.

I want to give a special note of appreciation to Guido Remmerswaal. While making this thesis, Guido always found time to help me as fast has he could, no matter how frustrating the issue. On every aspect of this thesis, Guido made sure that the optimum result was reached.

Finally I want to thank everybody who supported me throughout the process. Lau, thank you for supporting me all along the way and having to deal with any rough patches I experienced. Matys, thank you for helping me despite your busy schedule. To my friends and family I want to say thank you for all your love and help.

P.H.E. Voorn
Delft, June 2021

Acknowledgements

This work is part of the research programme AllRisk which is financed by the Netherlands Organisation for Scientific Research (NWO), project number P15-21 Project 4 (https://kbase.ncr-web.org/all-risk/project-groups/d-reliability-of-flood-defences/).

The Random Material Point Method simulations (Chapter 6) have been performed on Spider, a new high-throughput data-processing platform at SURFsara (https://www.surf.nl/high-performance-dataprocessing).

Abstract

Dikes protect people and lands all around the globe. With rising sea levels, the importance of well-designed dikes has never been more essential. One of the main factors that can compromise the stability of dikes are macro-instabilities. Macro-instabilities can cause dikes to lose their water bearing potential, leading to floods. Methods are developed to as accurately as possible determine the probability that a macro-instability takes place in order to prevent it. Therefore, recent advancements include the remaining strength after macro-instability, which may be able to prevent flooding.

The foremost methods to determine this remaining strength after macro-instability use D-Stability or the Material Point Method (MPM). Both D-Stability and MPM have advantages and disadvantages. D-Stability can quickly determine the probability that a macro-instability takes place, but can not model the process of failure, and must therefore simplify this process to estimate the remaining strength. MPM on the other hand can accurately model what happens after a macro-instability, but has a much larger computational cost, especially for probabilistic computations.

By supplementing D-Stability and MPM, this thesis proposes a method that exploits the advantages of both methods and mitigates the disadvantages. For a dike with a single clay layer, a connection was made between D-Stability and MPM, allowing dike profiles to be transferred back and forth. In order to make this connection, the SHANSEP undrained shear strength model was successfully implemented in MPM. By using the quick probabilistic D-Stability calculation and the post-failure modeling option of MPM, the probability of failure and the effect of failure can be quickly determined. By taking into account the effect of failure, the method can determine the probability of flooding, without simplifying the failure process. The method can also be used to determine if flooding via retrogressive failure or a larger single instability is more likely.

The method was tested via a case study and verified via a RMPM Monte Carlo analysis. For the case study, the probability of flooding was $5.189 \cdot 10^{-}3$ compared to an initial probability of failure of $7.22 \cdot 10^{-1}$, a reduction in the order of 139. This probability of flooding compared well to the probability of flooding of $5.308 \cdot 10^{-3}$ computed using the more accurate and computationally expensive RMPM. Based on these first results, the proposed method is a viable method to assess the probability of flooding after macro-instability for clay dikes.

Contents

List of Figures

List of Tables

List of Abbreviations and Symbols

- MPM = Material Point Method
- RMPM = Random Material Point Method
- OCR = Over Consolidation Ratio
- POP = Pre-Overburden Pressure
- SU = Undrained Shear Strength
- LEM = Limit Equilibrium Method
- FORM = First Order Reliability Method
- FoS = Factor of Safety
- PDF = Probability Density Function
- CDF = Cumulative Density Function
- GIMP = Generalised Interpolation Material Point Method
- WL = Water Level
- $P(I)$ = Probability of event I happening
- S_d = Sliding Force (N)
- R_d = Resisting Force (N)
- P_f = Probability of Failure
- Φ = Cumulative Normal Distribution
- β = Reliability Index
- μ = Mean
- σ = Standard Deviation
- Z = Limit State Function
- τ = Shear Strength (kPa)
- ψ = Dilatancy Angle (°)
- ϕ = Friction Angle (°)
- c = Cohesion (kPa)
- σ'_n = Effective Stress (kPa)
- γ = Unit Weight (kPa)
- S = Shear Strength Ratio
- m = Strength Increase Exponent
- P_f = Peak Factor

- R_f = Residual Factor
- ϵ_r^p = Residual Plastic Strain
- H_s = Softening Soil Parameter
- E = Young's Modulus (kPa)

1

Introduction

Globally hundreds of millions of people are protected by dikes against flooding. Rising sea levels pose a challenge to existing waterworks. For the lands and the people protected by waterworks, it is of vital importance that the design of these structures is as safe and future-proof as possible. To make sure that dikes are designed safely, it is required to model them as accurately as possible and to know as much about them as possible. New technologies in the field of dike design are being developed to increase our understanding of dikes and to model them as accurately as possible.

According to the Dutch safety regulations for the design of dikes, one of the main mechanisms that can cause dike failure, is macro-instability (ENW, 2017). When a macro-instability happens, a large part of the dike slides and compromises the water retaining potential of the dike. As technical possibilities advance, the precision to which the macro-stability of dikes can be determined advances along. The traditional method to determine the stability of a dike is via the limit equilibrium method (LEM). For LEM, the sliding and resisting forces are calculated over a circular plane in the dike. The circular plane where the ratio of sliding and resisting forces is the lowest, hast the lowest factor of safety and is the critical failure plane (USACE, 2003).

Via software, like D-Stability, LEM has been optimized to incorporate a new term: the probability of failure. The probability of failure takes into account the uncertainties of the soil parameters by using their parameter distributions. D-Stability makes this probabilistic calculation via a first order reliability (FORM) analysis (Van der Meij, 2020, Steenbergen et al., 2004). Although the FORM analysis gives a lot of information on whether a dike is stable or not, the post-failure behavior of dikes is not considered. LEM determines whether a dike is stable, but not what happens when a dike is unstable.

To determine what happens after failure, another method is developed. The the Material Point Method (MPM) is able to determine whether the dike is stable and what happens if the dike is unstable. The idea of MPM is that, by modelling the complete dike, not only the probability of failure can be determined, but also the probability of failure leading to flooding. That MPM is able to model large deformations in soil bodies has been proven (Andersen and Andersen, 2010, Martinelli et al., 2017). Because the dike is modeled completely, it should yield the most realistic results. The MPM model for dike stability is however still under construction and is computationally and analytically exhaustive to put into practice (Remmerswaal et al., 2018).

Both D-Stability and MPM offer a lot of possibilities for dike design and the assessment of dike macro-stability. However, the models are created independently and their development is also independent, which is limiting in the potential that a combination of both methods has. This thesis looks at how the technical advancements in both methods can be used complementary to exploit method specific advantages and mitigate method specific disadvantages. The result is a method that uses both D-Stability and MPM to better estimate the probability of flooding for dikes.

This section first states the problem that is to be solved. Second, the research questions are posed followed by the scope and limitations. An outline of the report is visualized in Figure 1.1.

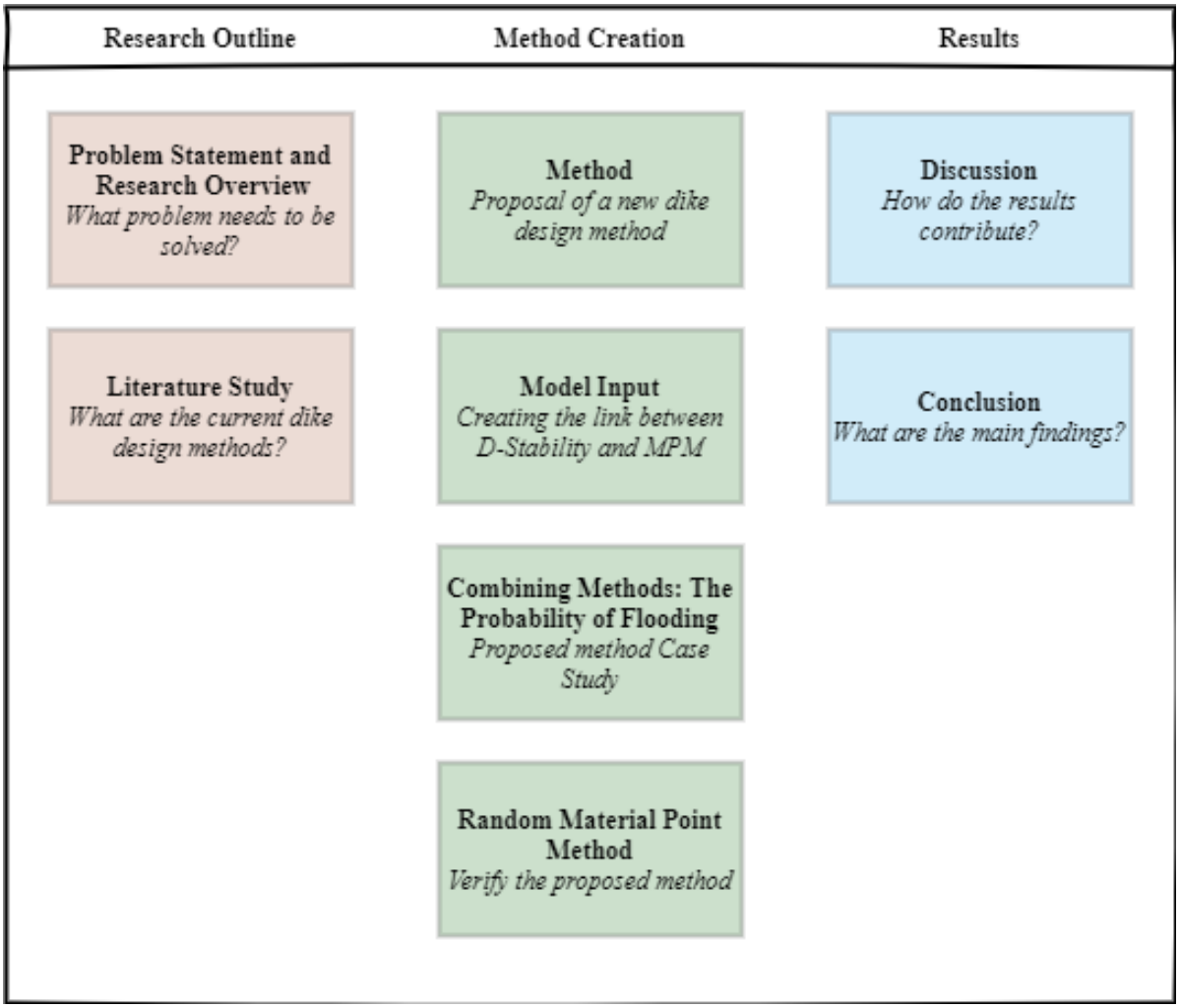

Figure 1.1: Research outline

1.1. Problem Statement

As new technologies emerge faster than engineering practice can keep up with, the calculations models for assessment of dike macro-stability do not always use their full potential. Promising methods based on probabilistics like the D-Stability FORM application and the Random Material Point Method have emerged relatively independently in the previous years with their specific advantages and disadvantages (Remmerswaal et al., 2018). Factors that influence the assessment for the different dike design methods include accuracy, speed and practical application. Where D-Stability is for example quick to assess the stability of dikes, the information that is given on the post-failure behavior of the dike is minimal. For D-Stability the speed and practical application are high, especially for probabilistic analyses, but the accuracy of mapping the post-failure behavior is low. On the other hand, for MPM, the speed and practical applicability are lower, but the accuracy is very high, as it gives a lot of information on the post-failure behavior. D-Stability is established as a widely used method for the assessment of macro-instabilities, while MPM is promising to be the future of dike design by its high degree of accuracy. Right now these calculation methods are operating independently while this is not directly required for engineering purposes. The aim is to use the speed of the D-Stability probabilistic potential with the accuracy of the MPM model, adding more information to the D-Stability model while reducing the computation time of the MPM model.

This thesis will look at ways to mitigate the disadvantages in current dike design methods and propose an improved method for dike design, using current methods complementary.

1.2. Research Questions

This section explores what questions need to be answered to solve the problem stated in Section 1.1. The main research question is defined as:

How can the probability flooding of a dike as a result of one or more macro-instabilities be efficiently estimated?

Sub questions to the Main Questions

1. What current methods exist for the calculation of residual dike resistance for dike macro-stability?
2. Can a method be created that uses the features of D-Stability and MPM supplementary?
3. Can the proposed method be used to predict the likelihood of different types of failure leading to flooding?
4. How do the results of the method compare to a RMPM Monte Carlo analysis?

1.3. Scope and limitations

To limit the scope of the research, several assumptions and simplifications are applied. The dike that will be investigated is a one-layered clay dike, where for simplicity the subsoil is modeled using the same material as the dike. The current MPM model uses the Von-Mises constitutive model which is most suitable for clay. Other soil models are still in development. In further research both of these factors can be expanded.

In this research, only the failure mode of macro-instability is considered. Flooding occurs if the dike is lower than the water level after a, or multiple, macro-instabilities have occurred. In reality there are more failure mechanisms of the dike that are likely to happen if the water level approaches the top of the dike, like overtopping. The increased chance of failure mechanisms other than macro-instability occurring for a weakened dike are not considered.

Assumptions and Limitations

- One-layered clay dike
- Water level at top of dike
- There are no other failure mechanisms

1.4. Outline

This section describes the setup of the thesis.

First, to see if improvements can be made in dike calculation models for macro-stability, it is of importance to first look at how the different calculation methods work. This investigation will be done in Chapter 2, the Literature Review. In the study different calculation methods will be explored to create a better understanding of their working and their possibilities and limitations.

Second, after the literature study, it is time to test the different methods for their practicality to map the limitations in practice. To do so a reference system has to be set up that creates a framework that is able to compare the different tests on their performance. This framework is made in Chapter 3. The input of the proposed method is should be standardized in order to compare the proposed method to other, existing methods. This standardization is done in Chapter 4 and verified by means of a sensitivity analysis.

Third, it is time to test the different methods by means of case studies. By performing the case studies the possibilities and limitations of each method can be tested and plotted. In Chapter 5, the different developed methods are executed and there results are compared.

After the results of the proposed methods are in, the results have to be verified. This will be done by a Random Material Point Method Monte Carlo analysis in Chapter 6. This is an extensive simulation of possible dike outcomes that is compared with the probability of flooding estimations by the proposed methods.

Lastly a discussion in Chapter 7 a conclusion in Chapter 8, and the recommendations in Chapter 9 will finalize the report.

2

Literature Review

The purpose of dikes is the prevention of floods. If a dike fails, it can lose the potential to prevent floods. Dike failure can take many shapes and forms and the potential failures are categorized in so-called failure modes, some of which are presented in Figure 2.1 (TAW, 1998). Failure modes consist of a starting mechanism, for example heavy rainfall, followed by a failure process leading to flooding. One of the failure modes is a macro-instability. For a macro-instability, a large part of the dike slides down. This shown in Figure 2.1 in C and E. Sliding of the inner or outer slope can cause a dike to breach and flood the nearby land. Conventional limit equilibrium methods determine the macro-stability of a dike by drawing a slip surface in the dike and then determine the ratio of forces along this slip surface to set the Factor of Safety (FoS) (USACE, 2003). However, the soil parameter values that determine the strength of the dike are often not known exactly. On top of that, the soil parameters may vary throughout the dike (Elkateb et al., 2003). This means that there is an uncertainty in the calculation of the factor of safety. When the range of possible soil parameter values and the most likely value are known, this is called the soil parameter distribution. The accuracy of the dike strength analysis can be increased by the soil parameter distribution via the First Order Reliability Method. In this analysis, the most likely combination of parameters leading to failure is determined (Van der Meij, (2020); Steenbergen et al., (2004); Jonkman et al., (2016)). Whether failure will occur can be assessed accurately via this method. What happens after failure is however less clear. The guidelines for assessment of this failure mode equate sliding of the inner slope, i.e. the starting mechanism, to dike failure to the flooding of the nearby land independent of the shape and size of the slip surface. This assessment is however not always correct, as sometimes the dike fails without flooding the nearby land (Van der Krogt et al., 2019).

A new method to take into account the post-failure behavior of dikes is by numerically modelling dikes. Numerical modelling in geotechnics has been proven to be effective in different types of analyses (Jing, 2003). For the numerical modelling of dikes, the Material Point Method is deemed the most suitable model, because of its ability to plot large deformations (Wang, 2017, Andersen and Andersen, 2010, Martinelli et al., 2017). The method has the potential to very accurately model the dike behavior, but still has some disadvantages. MPM is still under development and the use of the model is not yet common practice. Next to that is MPM computationally and analytically exhaustive, especially for probabilistic analyses (Remmerswaal et al., 2018).

D-Stability and MPM make up the state of the field for dike design. This section will dive deeper into the workings of both methods and elaborates on the advantages and disadvantages of both methods.

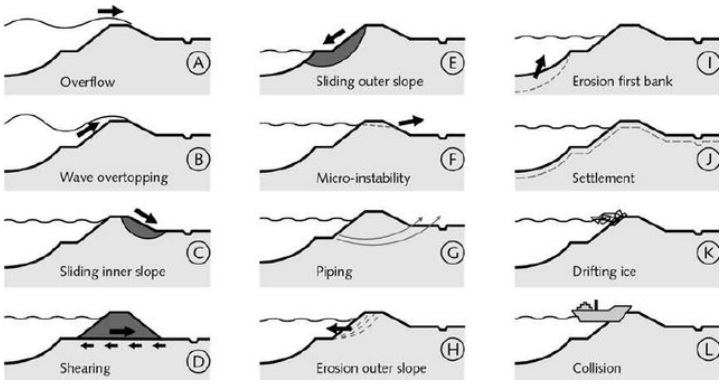

Figure 2.1: Failure modes for dikes (TAW, 1998)

2.1. Probabilistic Dike Design

There are several degrees of accuracy for which the stability of a dike can be determined, which are typically divided in five levels (Jonkman et al. 2016). There are less complex methods with a lot of assumptions, thereby requiring large safety margins, while more complex methods compute the probability of failure or even the associated risk. The levels from least precise (Level 0) to most precise (Level IV) are:

- **Level 0:** Deterministic analysis using mean values of random properties.
- **Level I:** Semi-probabilistic analysis approximating failure probability using characteristic values of random properties based upon mean values and predefined partial factors.
- **Level II:** Numerical approximation of failure probability using linearized limit states and normally distributed random properties.
- **Level III:** Full numerical integration of the failure probability (for example Monte Carlo method)
- **Level IV:** Risk-based calculation which incorporates failure probability and consequences.

Level 0
A Level 0 calculation is the most basic type of dike design calculation. The mean values for the different parameters are determined and a deterministic LEM analysis is performed. The result is a factor of safety along a sliding plane.

Level I
For Level I calculations a probabilistic aspect is added to the calculation by using design values. Generally when the safety of a dike is assessed following a Level I probabilistic design, a sliding plane is determined and a design load S_d and a design resistance R_d are used for the calculations. The design values are retrieved by looking taken a conservative percentile of the distribution (Jonkman et al., 2016). The result of this type of calculation is a conservative safety factor.

Level II
If the acting resisting forces (R) are lower than the load (S) acting on a specific dike surface, failure occurs. However, the values for R and S are never known for certain. Both the resisting forces as the load are dependent on a set of parameters which vary through time and space. To account for this variance in parameters, the concept of Probability of Failure exists. The Probability of Failure (Pf) is the probability that the resisting forces are smaller than the load, or in the form of an equation (2.1) (Jonkman et al., 2016):

$$P_f = P[S > R] \tag{2.1}$$

From this basic principle, the probabilities of more complex situations can be estimated in a limit state analysis. The limit state is defined as equation 2.2.

$$Z = R - S \tag{2.2}$$

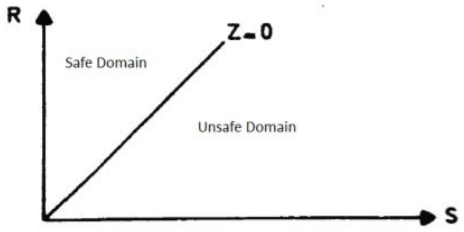

Figure 2.2: Limit state visualization (Jonkman et al., 2016)

When equation 2.2 turns out negative, failure occurs. This principle is visualized in Figure 2.2 by Jonkman et al. (2016)

To generalize the limit state equation to encompass all variables that make up the resistance and the load, the equation for the limit state becomes as in equation 2.3, where all variables are stored in the $\underline{X}$ symbol.

$$g(\underline{X}) = Z = 0 \tag{2.3}$$

To take account for all the variables stored in $\underline{X}$ and their variability, this equation takes yet a new form. The variables that make up $\underline{X}$ have a probability density function that can be described by $f(x)$. For all the probability density functions for all the variables, the probability of failure takes the new form of 2.4:

$$P_f = \int_{g(\underline{X})<0} f_{\underline{x}}(\underline{x}) d\underline{x} \tag{2.4}$$

The effect of this integration can best be visualized by Figure 2.3. The lines of equal probability are altitude lines of function f_{RS}, the combined 3D probability density function of f_R and f_S. The volume of the probability function f_{RS} that is situated in the unsafe domain determines the probability of safety for the system.

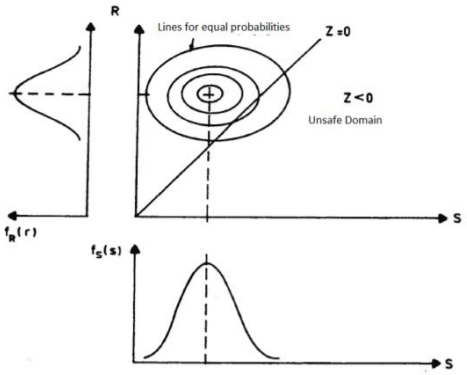

Figure 2.3: Lines of equal probability in the limit state plane (Jonkman et al., 2016)

Directly linked to the probability of failure is the Reliability Index (β). Instead of indicating how unstable a structure is, the reliability index indicates how secure a structure is. The reliability index is directly linked to the probability of failure in accordance to $P_f = \Phi(-\beta)$, where Φ is a cumulative normal distribution (Jonkman et al., 2016). For a linear system with normal distributions of the different parameters, the reliability index is defined as equation 2.5 from Jonkman et al. (2016).

$$\beta = \frac{\mu_z}{\sigma_z} \tag{2.5}$$

However, not all limit state equations are linear. To calculate the failure probability for non-linear limit state equations, the limit state equation needs to be linearized for which a Taylor expansion can be used (Jonkman et al., 2016). This linearization however causes an error in the calculation which decreases the reliability of the calculation. This linearization in done in the design point. The effects of this linearization can be seen in Figure 2.4. The limit state function is linearized in the design point to more easily calculate the integral of the function.

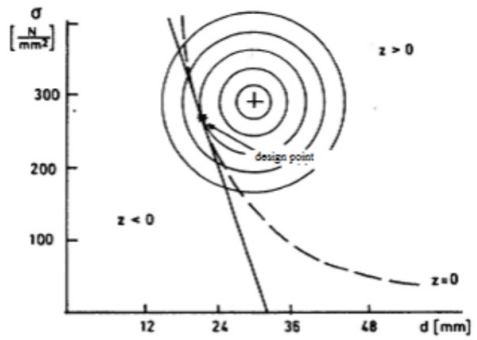

Figure 2.4: Effect of linearization in the design point (Jonkman et al., 2016)

Level III
For the numerical approach of a level III calculation, the same steps as in the Level II approach can be followed. The basic premise is that equation 2.4 is solved and the volume of the different parameters in the unsafe domain is found. However, where for a level II method the limit state function is linearized in the design point, the Level III method explicitly solves the integral of function 2.4. This integral with functions $f_R(x)$ and $f_S(x)$ can be solved in two ways according to equations 2.6 and 2.7.

$$P_f = \int_{-\infty}^{+\infty} F_R(x) f_s(x) dx \tag{2.6}$$

$$P_f = \int_{-\infty}^{+\infty} f_R(x)[1 - F_s(x)] dx \tag{2.7}$$

The way to solve these functions numerically is via splitting the volume $Z < 0$ in small volumes (Jonkman et al., 2016). This is possible via function 2.8. The result of this formula can be observed in Figure 2.5.

$$P_f = \sum_i \sum_j f_{R,S}(r_i, s_j) \Delta r \Delta s \tag{2.8}$$

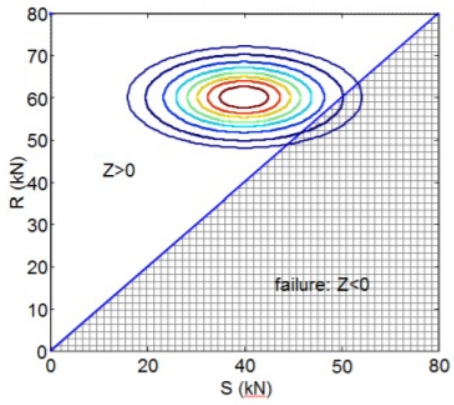

Figure 2.5: Numerical integration level III (Jonkman et al., 2016)

This method of obtaining the probability of failure is however computationally very exhaustive. Especially when more variables are added to the analysis. The explicit numerical approach for the probability of failure is therefore mainly suited for a situation with two variables in the integral. A way to numerically solve this problem for more variables is by means of a Monte Carlo analysis. Via a Monte Carlo approach the function is solved for different parameter values selected randomly each time according to their mean an standard deviation. This way a percentile of the solutions will be located in the unsafe domain which then makes up the probability of failure. A visualization of this process is given in Figure 2.6. The dots falling into the unsafe domain make up the probability of failure.

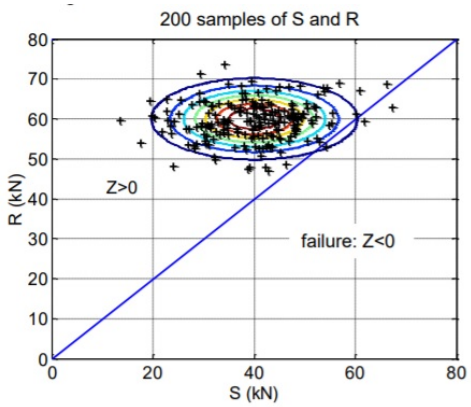

Figure 2.6: Domain results Monte Carlo method (Jonkman et al., 2016)

Level IV

The most complex dike stability calculation is the Level IV calculation. The premise is similar to a Level III calculation but now the effect of failure is incorporated into the analysis as well. Based on the predicted effect of failure, dikes can be designed more efficiently. If the consequences of failure are low, the dike design can be made less conservative, and therefore less costly.

2.2. D-Stability Dike Assessment

D-Stability is one of the most widely used programs for the macro-stability assessment of dikes. The main advantages are that is is quick and user friendly. The main disadvantage is that little is known on the post-failure behaviour. To explain how D-Stability works, first the Limit Equilibrium Method that forms the basic principle behind D-Stability is explained. Second, the Soil Models used by D-Stability are discussed. Lastly the calculation potential is explained and the options are discussed in increasing order of complexity.

2.2.1. The Limit Equilibrium Method

Currently one of the most commonly used methods to assess the stability of dikes is via software that uses the Limit Equilibrium Method (LEM). This method assess what is the most likely slip plane among which failure occurs, and takes the ratio between the resisting and driving forces to calculate the factor of safety. Several methods exist to determine what the critical slip surface is over which failure is most likely to occur. The methods D-Stability offers to determine this critical slip surface are the Bishop, the Uplift Van and the Spencer models. These models divide the soil body into slices and compute the forces per slice. The Bishop model plots a circular slip plane, the Uplift-Van model plots a dual-circular slip plane (Van der Meij, 2020). The Uplift-Van model is especially used when a permeable layer underneath the dike can cause uplift near the toe of the dike (Van der Meij, 2020). Instead of a circular slip plane, the Spencer model uses a set of points through the dike with straight lines in between (Van der Meij, 2020). The points be determined freely to alter the slip plane. An example of the division into slices according to the Bishop model is provided in Figure 2.7. The main advantages of this method are that it is relatively easy to implement and the computational time is rather low. The disadvantage is that assumptions have to be made concerning the location and shape of the slip surface and henceforth the reliability decreases. The dike stability can be expressed in the factor of safety in the deterministic and semi-probabilistic approach, but can also be expressed as the probability of failure via the Level II probabilistic First Order Reliability Method (FORM).

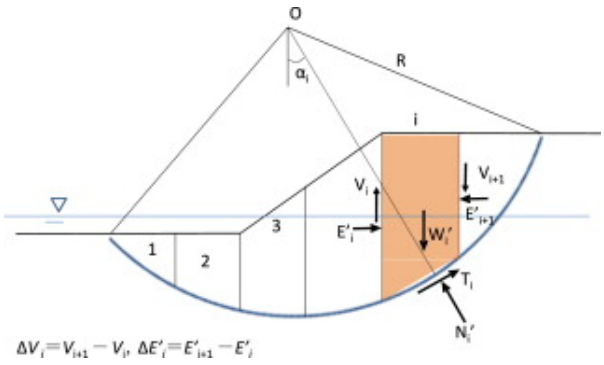

Figure 2.7: Division into slices by D-Stability (Tsuchida and Athapaththu, 2015)

2.2.2. Shear Strength Models

For the Limit Equilibrium Method the strength of the soil is calculated over a certain sliding plane. The way to calculate the strength of the soil at a certain location is different for different materials. This is why D-Stability has the option to select the C-Phi model for drained materials like sand, and the SHANSEP model for undrained materials like clay (Van der Meij, 2020).

C-Phi Model with Dilatancy

The formula for the drained material shear strength according to the C-Phi model is given in Equation 2.9 and the parameters are given in Table 2.1.

$$\tau = c \times \frac{\cos\psi \times \cos\phi}{1 - \sin\psi \times \sin\phi} + \sigma'_n \times \frac{\cos\psi \times \sin\phi}{1 - \sin\psi \times \sin\phi} \tag{2.9}$$

Equation 2.9 has three variations. The fist variation is when the friction angle is equal to the dilation angle $\psi = \phi$. This is called associate behavior (Van der Meij, 2020). The resulting failure criterion is the Mohr-Coulomb failure criterion, which is given by Equation 2.10.

$$\tau = c + \times \sigma'_n \times \tan\phi \tag{2.10}$$

The second variation is non-associated behavior. Here the dilatancy angle is not equal to the friction angle ($\psi \neq \phi$). In this case, the formula of Equation 2.9 is used.

The last variation is when the dilatancy angle is zero ($\psi = 0$). In this case, the shear strength is given by Equation 2.11

$$\tau = c \times \cos\phi + \sigma' \times \sin\phi \tag{2.11}$$

Input Parameter	**SI**
Unit Weight (γ)	kN/m^3
Cohesion (c)	kN/m^2
Friction Angle (ϕ)	◦
Dilatancy Angle (ψ)	◦

Table 2.1: Mohr-Coulomb model input

SHANSEP model

The shear strength model for undrained materials is the SHANSEP model. The SHANSEP model calculates the shear strength of the soil based on the current and previous stress experienced by the soil. The yield stress (σ'_y) is calculated by either adding the pre-overburden pressure parameter (POP) to the vertical effective stress (σ'_v) or by multiplying the vertical effective stress with the over consolidation ration (OCR) as given in equations 2.12 and 2.13 (Van der Meij, 2020). The formulas for the shear strength are given by Equations 2.12, 2.13, 2.14 and 2.15. The parameters are given in Table 2.2.

$$\sigma'_y = \sigma'_v + POP \tag{2.12}$$

$$\sigma'_y = \sigma'_v \times OCR \tag{2.13}$$

If $\sigma'_v > 0$:

$$\tau = s_u = \sigma'_v \times S \times \frac{\sigma'_y}{\sigma'_v}^m \tag{2.14}$$

If $\sigma'_v = 0$:

$$\tau = s_u = 0 if \sigma'_v = 0 \tag{2.15}$$

Input Parameter	**SI**
Unit Weight (γ)	kN/m^3
Shear Strength Ratio (S)	[−]
Strength Increase Exponent (m)	[−]
Pre-Overburden Pressure (POP)	kN/m^2

Table 2.2: SHANSEP shear strength model input

2.2.3. Semi-Probabilistic D-Stability Calculation

In the current Dutch safety standard, the first geotechnical failure is equated to the failure of the dike (ENW, 2017). According to this standard, the probability of failure of a dike is equal to the probability of the first instability. For basic calculations, D-Stability determines a slip surface and over that surface the load and resistance are determined. The ratio of these values finally determines the safety factor. The result of an example calculation can be seen in Figures 2.8 and 2.9. This standard calculation is based on parameter values determined by their design values. In the Dutch guidelines, the factor of safety then needs to be converted to a probability of failure (ENW, 2017).

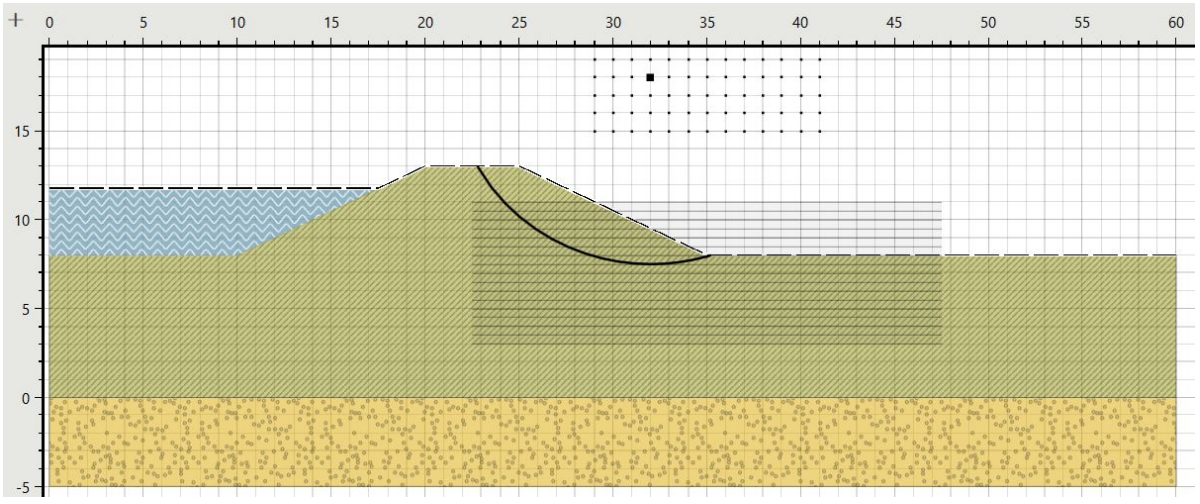

Figure 2.8: Example Bishop calculation in D-Stability

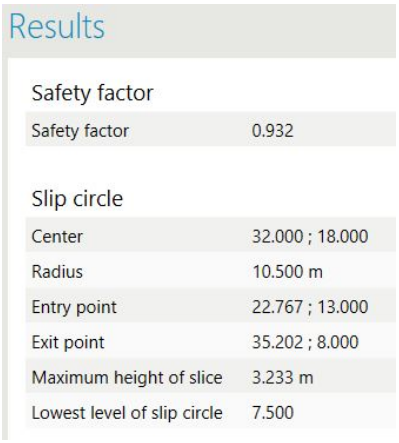

Figure 2.9: Results of example Bishop calculation

2.2.4. Probabilistic (FORM) D-Stability Calculation

The probability of failure can be determined via a more advanced option that D-Stability offers besides the standard safety factor calculation: FORM probabilistic calculation. For this calculation, the predetermined cross-section for which the factor of safety is determined, must be used and the variance of the parameters must be defined. The program then will try to solve the integral for the parameter combinations that fall into the unsafe area. The shortest distance from the mean parameter values to the failure zone then indicates the highest probability of failure. The results of such a calculation can be observed in Figure 2.10.

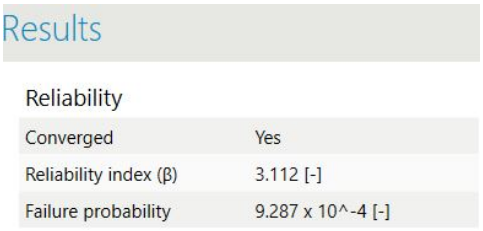

Figure 2.10: Results probabilistic calculation D-Stability

The probability of failure can thus be calculated by varying the different parameters over the predetermined slip surface of the dike. This can be done for one particular water level but a fragility curve can be created by performing the calculation multiple times. In this way the reliability (β) can be plotted against the water probability density curve.

2.2.5. Probability of Flooding using D-Stability

In the Netherlands dikes are designed according to the economic and societal risks they bear (ENW2017) (Kok et al.2016). According to Van der Krogt et al.(2019), the main societal and economical risks can be equated to the risk of flooding. Risk is defined as the probability times the consequences. According to this definition of risk, not only the probability of failure should be used for dike design, but also the consequences of that failure should be incorporated. To make a candid design, it is therefore of interest to analyze what failure amounts to if failure happens. To improve the dike design to follow the new standards, it is helpful to know what the situation will be after a dike has failed and whether flooding will occur. With the addition of the criterion of flooding in case of failure, the designed reliability of dikes increases. This principle is clearly explained in the paper of Van der Krogt et al. (2019). The probability of flooding is dependent on the water level. The first instability can lead to flooding in case of high water levels, however, if the water levels are low, flooding does not occur. If a second instability occurs after the first instability, flooding can again either occur or not occur. The probability of flooding is then dependent on the first instability, the water level in the first instability, the second instability and the water level at the second instability. This "probability tree" continues until failure does occur. This process is schematized in Figure 2.11 as made by Van der Krogt et al.(2019). Flood only occurs if a combination exists between an instability and a certain water level.

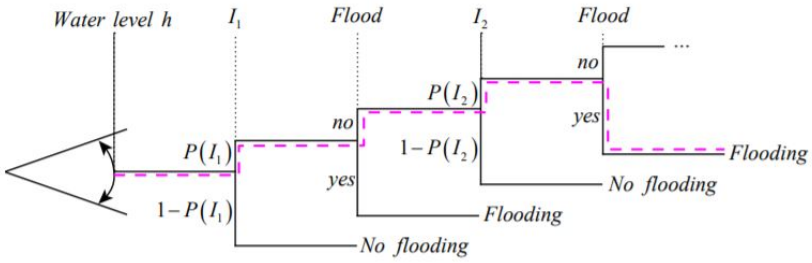

Figure 2.11: Probability of flooding by successive instabilities (Van der Krogt et al., 2019)

The probability of failure of the dike is dependent on the probabilities of the successive instabilities. This means that instead of equating the probability of failure for the dike to the probability of failure for the first instability $P(F) = P(I_1)$, the probability of failure, as visualized in the event tree becomes as in Equation 2.16 (Van der Krogt et al., 2019).

$$P(F) = P(I_2|I_1 \cap I_1) \tag{2.16}$$

This equation takes the general form for the probability of flooding due to n successive instabilities as Equation 2.17 (Van der Krogt et al., 2019).

$$P(F) = P(\cap_{i=1}^{n} I_i) = P(\cap_{i=2}^{n} I_i|I_{i-1}) \cdot P(I_1) \tag{2.17}$$

Conditional to the water level (defined as h), the equation for the probability of flooding after n successive instabilities, takes the form of Equation 2.18 (Van der Krogt et al., 2019).

$$P(F|h) = P(\cap_{i=1}^{n} I_i|h) = P(\cap_{i=2}^{n} I_i|I_{i-1}, h) \cdot P(I_1|h) \tag{2.18}$$

All failure probabilities for the successive instabilities in combination with the water levels, constitute the real probability of flooding for the dike. To compute the probability of flooding, the successive instabilities should be carefully calculated since the situation after an instability is used as a new situation. Flooding can also occur at the first instability. For this to happen, the dike must fail according to a specific failure plane at a specific water height. This calculation gives a probability of flooding for the first instability. It is possible that this probability of flooding via the first macro-instability is higher than the probability of flooding by successive instabilities (Van der Krogt et al., 2019). For every situation in the dike failure process, the probability of failure and the probability of flooding should be calculated until both have the same values.

2.2.6. Water Level

To analyze the probability of flooding, the water level is of key importance. To incorporate the water level in the analysis, a Gumbel maximum annual water level distribution is used. In the Gumbel distribution, the probability of the water level reaching a specific height per year is determined (Gumbel, 1941). The distribution is given by Equation 2.19.

$$\frac{1}{\beta} e^{-(z+e^{-z})} \tag{2.19}$$

2.2.7. Probabilistic Results - Fragility Curves

Different dike cross-sections yield to different probabilistic results. To get a good overview of the probabilities of different dike instabilities, fragility curves are used. In a fragility curve, the reliability index of an instability is plotted against a dominant load value, in this case the water level (Schweckendiek et al., 2017). The result is an overview of which probabilities of (successive) instabilities per water level. The probability of the water level can either not be incorporated, like in Figure 2.12 or be incorporated in the curves, like in Figure 2.13. In Figure 2.12 it can be seen that the first instability (I_1) has the same probability independent of the water level. The second instability (I_2) however becomes less likely for higher water levels after the first instability has occurred. In Figure 2.13 it can be seen that if the water level is taken into account in the curves, the probability of the first instability becomes less likely for higher water levels, since higher water levels are less likely.

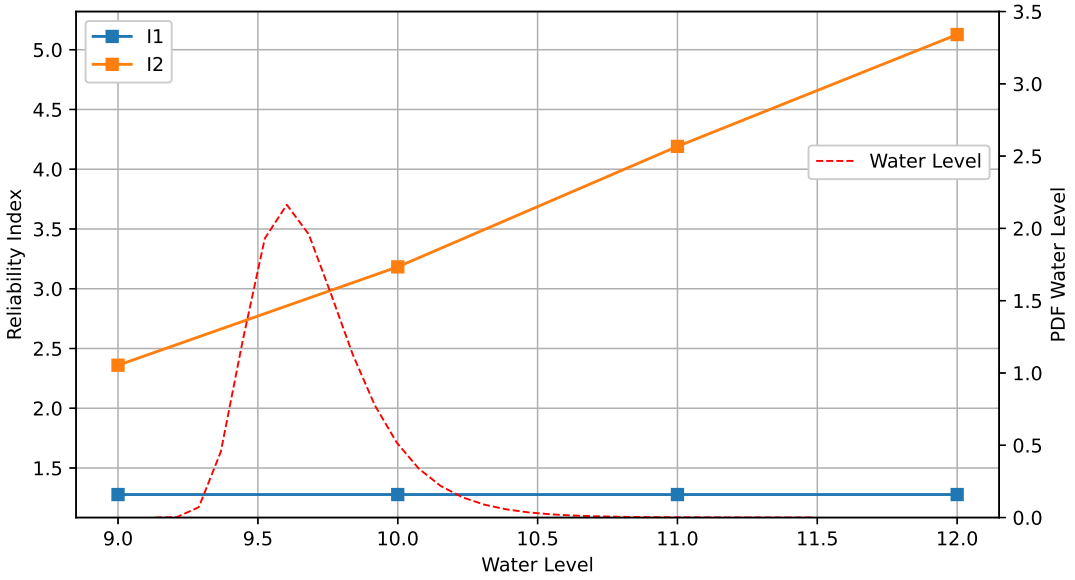

Figure 2.12: Example fragility curves: water level probability not applied

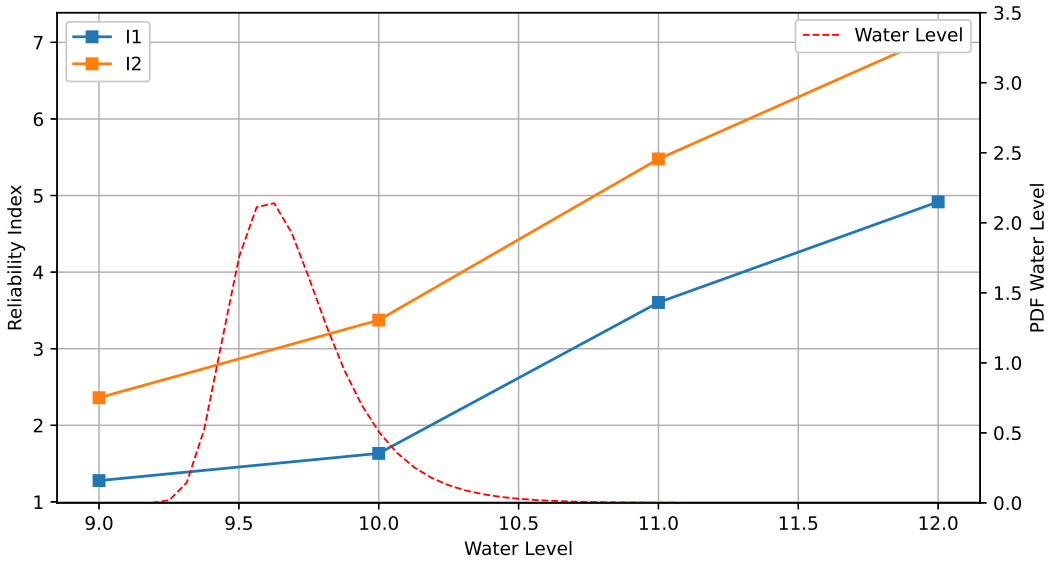

Figure 2.13: Example fragility curves: water level probability applied

2.3. The Material Point Method (MPM)

The latest development in the assessment of the macro-stability of dikes is the Material Point Method (MPM). This method plots all the stresses and strengths in the dikes and assesses the dike stability. The advantage is that a very precise model is used and a lot of information is given on the post-failure behavior. The disadvantage is that a probabilistic analysis takes very long and that the model still has some errors. This section covers the workings of the method and the problems that are still being solved.

2.3.1. Background of MPM

To understand how the residual strength of dikes can be computed by the Material Point Method, it should be clear how the method operates in order to assess its applicability for determining the dike strength. The MPM is an adaptation of the Finite Element Method (FEM). The principle of both numerical methods is that in a grid the state variables can be plotted and used to calculate other variables. The grid can be created in such a way that it represents a soil body or in the case of this research, a dike. For original FEM, the grid is structured based on nodes and integration points. The nodes form the corners of the grid elements and the integration points lay on specific predetermined places inside these elements. With the information stored on the nodes, the governing equations that determine the material behavior are solved on the integration points. After the equations are solved in the FEM, the mesh is updated to a new position and the process is repeated. A visual representation of the nodes and the integration points for the FEM is given in 2.14. The red dots represent the integration points and the yellow dots represent the grid nodes.

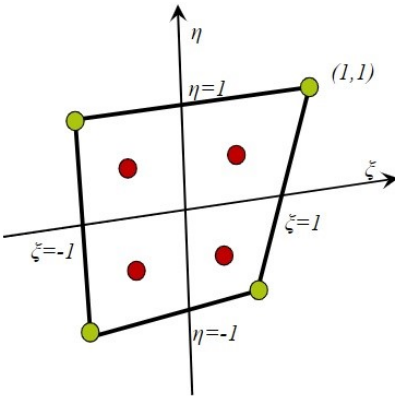

Figure 2.14: Integration points inside grid element for FEM (Vardon, 2018)

Where the FEM uses integration points to solve the governing equations, the basic premise of the MPM is the use of the so-called "material points." These material points have the ability to move freely throughout the mesh. This is the main difference with the FEM where the integration points are stationary within the element. In FEM, when plotting large deformations, the mesh gets distorted. For the MPM, the mesh itself resets after each computation of the stresses. This process is visualized in Figure 2.15 (Wang et al., 2015). In the first phase of the process, the information of the material points is mapped to the background mesh. The mesh is then updated on account of the solving of the equation of motion. In the last step the material points are updated by the new distorted mesh and the mesh is restored to its original position from which the process repeats itself. Information is transferred and re transferred from the material points to the grid nodes back and forth (Wang et al., 2015).

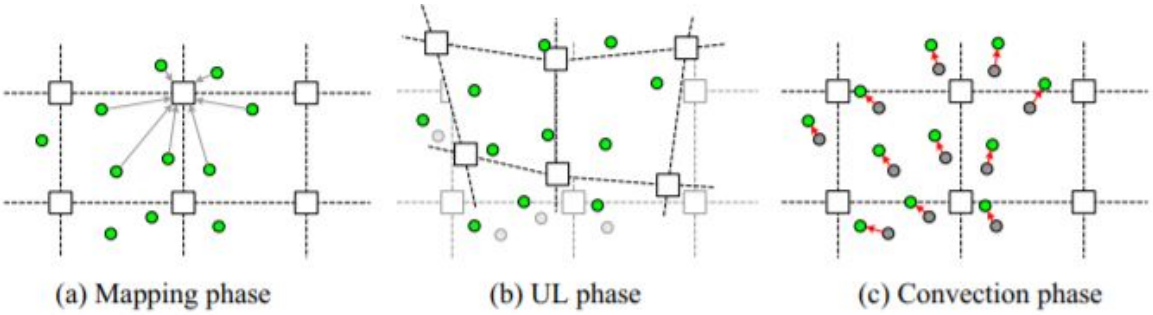

Figure 2.15: MPM mesh updating (Wang et al., 2015)

2.3.2. Implicit MPM

Via mapping and remapping, the governing equations need to be solved to know the development of the stresses and strains in the grid. The current state of the field MPM that is under development is the implicit method of solving the governing equations. The set of governing equations that needs to be solved for the

model is given by the conservation equations for mass and momentum given by: 2.20 and 2.21 where **v** is the velocity, $\boldsymbol{\sigma}$ is the Cauchy stress and **b** is the body force (Wang et al., 2015).

$$\frac{d\rho}{dt} + \rho\nabla\cdot\mathbf{v} = 0 \tag{2.20}$$

$$\rho\frac{d\mathbf{v}}{dt} = \nabla\cdot\boldsymbol{\sigma} + \mathbf{b} \tag{2.21}$$

Through mathematical derivations, the numerical form of the governing equation in static form is given by equation 2.22.

$$\boldsymbol{K^t\overline{u} = \overline{F}_{ext}^{t+\Delta t} - F_{int}^t} \tag{2.22}$$

In this equation, K^t is the stiffness matrix that is comprised of a linear part, $\boldsymbol{K_L^t}$ and a non-linear part $\boldsymbol{K_{NL}^t}$. $\boldsymbol{\overline{u}}$ Is the incremental displacement and $\boldsymbol{F_{ext}^{t+\Delta t}}$ is the external force at time $\boldsymbol{t+\Delta t}$ and $\boldsymbol{F_{int}^t}$ is the internal force at the time $\boldsymbol{t}$. This static equation can be converted to a dynamic form by adding an inertial term $\boldsymbol{M^t a^{t+\Delta t}}$ to the left side of equation 2.22. When rewriting the equation, a new stiffness matrix emerges in the form $\boldsymbol{\overline{K^t}}$ and a new external force emerges in the form $\overline{F}_{ext}^{t+\Delta t}$. In the inertial term $\boldsymbol{M^t}$ the mass matrix at time $\boldsymbol{t}$ and $\boldsymbol{a}$ is the acceleration at time $t+\Delta t$ (Wang et al., 2015).

$$\boldsymbol{\overline{K}^t\overline{u} = \overline{F}_{ext}^{t+\Delta t} - F_{int}^t} \tag{2.23}$$

This term can even be expanded by adding a term for damping on the right side of the equation defined as $\boldsymbol{F_{damp}^{t+\Delta t}}$ at time $\boldsymbol{t+\Delta t}$. The derived equations help to fill the created mesh with soil properties

2.3.3. Stress Oscillations

One of the main problems the MPM model still faces is the presence of stress oscillations. According to González Acosta et al., (2020), these stress oscillations are a caused by "a combination of poor force and stiffness integrations, stress recovery inaccuracies, and cell crossing problems". One of the main contributing factors is the error caused by the use of (discontinuous) bi-linear shape function gradients (González Acosta et al., (2020). This means that the mapping of the material points on updated nodes, which happens if the material points move through the grid, becomes inaccurate. González Acosta et al. (2020) proposes several solutions to this problem. The main solution, which is also implemented in the MPM model used in this thesis, is the "generalised interpolation material point method (GIMP)". In the GIMP method, "finite element shape functions are replaced by functions constructed based on the linear finite element shape functions and a material point support domain", meaning that the "material point has a domain over which its influence is distributed" (González Acosta et al. 2020). Several other methods are also proposed by González Acosta et al. (2020) and are currently being implemented into the MPM model. The presence of these stress wave however does indicate that the model is still under construction and not completely user ready.

2.3.4. Pore Water Pressure

Another aspect that indicates that the MPM model is still under construction, is the absence of the pore water pressure in the model. For an accurate modelling of the soil stresses, the modelling of the pore water pressure is essential. In some MPM models the pore water pressure has been incorporated and is used to model liquefaction behavior (Ghasemi et al. 2018). The MPM model used in this thesis, being under development, has not incorporated the pore water pressure yet, but will incorporate it in the future. The result for the dike analysis is that dike failure due to pore pressure build-up cannot be modelled exactly.

2.3.5. Constitutive Behavior

Additional to these governing equations, to compute the stresses and strains in the subsurface the constitutive behavior of the soil needs to be described. Several constitutive models exist to approximate the stress-strain behavior of different types of soils. However, not all these models are yet suitable to be used in MPM, partially due to the previously mentioned stress oscillation. In the current stage of the research on RMPM, a linear elastic, cohesion softening Von Mises model can be applied (Wang et al., 2015). The basis premise of this model is that the strains are divided into an elastic part ϵ_E and a plastic part ϵ_P and that the soil becomes weaker as the plastic strains increase. The elastic strains are assumed linear and the plastic strains occur

when the stresses form such a combination that the yield surface of the model is reached. This yield surface is defined by Equation 2.24 and looks like Figure 2.16.

$$F_{vm} = \frac{\sigma_1 - \sigma_3}{2} - C_u \tag{2.24}$$

If $F_{vm} = 0$ the material reaches its yield surface and plastic strains occur. The cohesion softening part of the model explains that the soil loses strength as the plastic strain invariant increases. When the system of equations is solved over the mesh, a failure surface emerges at the location where the plastic strains are largest. Along this surface the dike fails for a given set of parameters. An example of such a failure surface is given in Figure 2.17. In the figure it is clearly visible that where the plastic strains are the highest, the soil weakens according to the cohesion softening aspect of the Von Mises model. The location of the highest plastic strains in the mesh is what determines the shear banding that occurs and that is visible especially in Figure 2.17a.

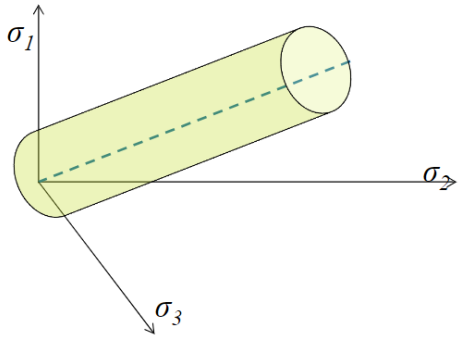

Figure 2.16: Von Mises failure surface (van den Eijnden, 2018)

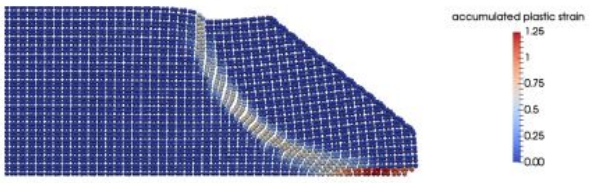

(a) Shear band formed due to toe excavation

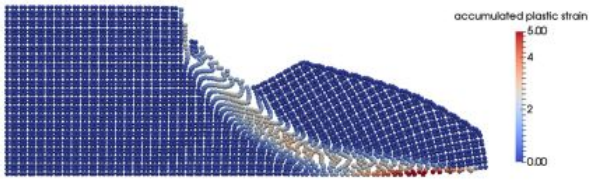

(b) Final configuration of collapsed slope

Figure 2.17: Failure surface MPM (Wang et al., 2015)

2.3.6. Soil Softening

In the Von Mises model, soil softening is considered. This means that, as the stresses develop in the subsoil, the soil loses part of its strength. In the model this is done by setting limitation to how much of its strength the soil loses and how quickly the soil loses its strength. The relation can be described by the initial shear strength (SU_0) the residual shear strength (SU_{Res}), the softening parameter (H_s) and the residual factor. Adjusting these input parameters means adjusting the experiences softening of the dike and thus the macro-stability of the dike. In Chapter 4 the exact values of these parameters are determined.

$$\bar{\epsilon}_r^p = \frac{r_f c_0 - c_0}{H_s} = \frac{(r_f - 1)c_0}{H_s} \tag{2.25}$$

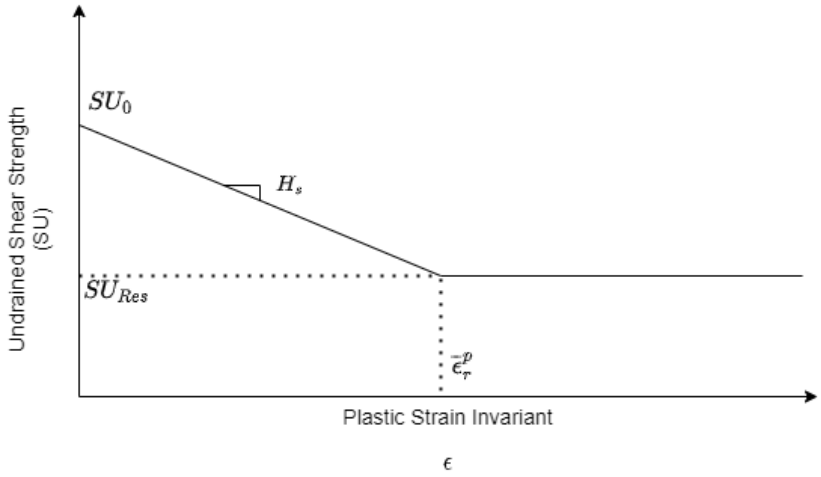

Figure 2.18: Softening modulus (H_s) in cohesion softening model (Wang, 2017)

2.4. The Random Material Point Method

A probabilistic variant of the Material Point Method is the Random Material Point Method. The Random Material Point Method uses a Level III approach to determine the probability of failure. The standard way of determining the probability of failure for numerical models is via a Monte Carlo analysis. This method uses the distribution of parameter values as input for the calculation of the dike strength. By calculating the dike strength with the varying parameters for a number of times (for example 10.000) a distribution of safe and unsafe dikes can be obtained. From this range of answers the probability of failure can be selected as a portion of the unsafe results in the analysis.

2.4.1. Spatial Variability

Parameter variation can take two main shapes. For the limit equilibrium method, parameters are generally varied homogeneously. This means that a LEM model uses one particular clay parameter value per soil layer. For example, if the friction angle of clay has a normal distribution with mean value $\mu = 10^\circ$ and a standard deviation of $\sigma = 4^\circ$, a calculation can occur where the friction angle ϕ is 8°. This means for the LEM calculation that the entire clay layer is assumed to have a friction angle of 8°. The soil body is assumed homogeneous.

In reality however, soils are not homogeneous. Most soils, especially sedimentary soils, have a degree of layering have a degree of layering, even within the classified soil layers, where weaker zones are interchanged by stronger zones. The location of these layers can vary and this variation can influence the failure surface and strength of the dike. A weak layer in a lower part of the dike can increase the probability of flooding of a dike significantly. The concept of strength variation within a soil layer is called "soil heterogeneity." Whereas it is not yet possible to model this soil heterogeneity with the LEM, the RMPM makes this possible. Soil drillings determine as precisely as possible to determine the space between consecutive weak layers to assign an horizontal and vertical correlation coefficient θ_v and θ_h. Based on these factors, the layering in the dike is then randomized by the distribution of the parameters within the layer according to their correlation.

2.4.2. Probability of Flooding using the Random Material Point Method

In terms of flooding this method can be used to reevaluate the strength of the dike after successive instabilities. The point of dike failure is not equated to the first instability, but is determined by the water level reaching the top height of the dike (Remmerswaal et al. (2018)). One of the parameters that can be varied in the equation, is the water level. By varying the water level, the Monte Carlo simulation takes into account the water level and recognizes flooding when the water level supersedes the residual dike height.

2.5. Conclusion

D-Stability and the MPM model are the two main methods exist for the calculation of dike macro-stability.

D-Stability is established as a robust, user-friendly model for a quick assessment of the dike stability. Next to a deterministic calculation, the model can perform quick probabilistic calculations on based on the FORM

method. The disadvantage of the method is the lack of information on the post-failure behavior and the disability to account for soil heterogeneity.

MPM is very suitable for the modelling of the dike macro-stability. The MPM model computes the exact stresses and strains in the dike and is able to plot the post-failure behavior. Another advantage of the MPM model is the option to model soil heterogeneity. Via a RMPM Monte Carlo analysis, a probabilistic dike assessment can be made that takes into account the natural layering of the soil. The disadvantages of MPM are that the model is still under construction and the duration of the analysis. A full RMPM Monte Carlo analysis can take several days to compute. Especially for lower failure probabilities, the analysis is very time consuming.

In the next chapter a method is proposed that aims to exploit the advantages of both methods and mitigate the disadvantages.

3

Method

In this chapter a method is proposed to estimate the probability of flooding by combining D-Stability and MPM. Elements of these models are connected to exploit the best characteristics of both. This chapter explains how the methods were combined, which calculations are involved and which assumptions have been made. Chapter 4 will go further into detail on the input parameters for the method.

3.1. Method Components

The proposed method is made up out of several parts. For clarification, the different parts that make up the method are briefly explained in this section. The connection between D-Stability and MPM consists of a D-Stability calculation, a MPM calculation and uses fragility curves to plot the results.

3.1.1. D-Stability Probabilistic Calculation

The D-Stability calculation consists of a few steps. First, the input parameters are determined. For a clay dike, the SHANSEP model is used and the SHANSEP input parameters are: the Shear Strength Ratio (S), the Strength Increase Exponent (m), the Pre-Overburden Pressure (POP). The soil unit weight is used to determine the soil stresses. The input in D-Stability is for all the SHANSEP input parameters (m, S and POP), is a mean and a standard deviation for a normal distribution. Using the Bishop model, a deterministic calculation is performed to determine the factor of safety and the slip surface with the lowest factor of safety. On that slip surface a First Order Reliability Method (FORM) then calculates the highest probability of failure. The probability of failure is determined by calculating the most likely combination of parameters leading to failure. The result is a probability of failure and a combination of parameters for which failure is most likely to happen. This combination of parameters is the design point.

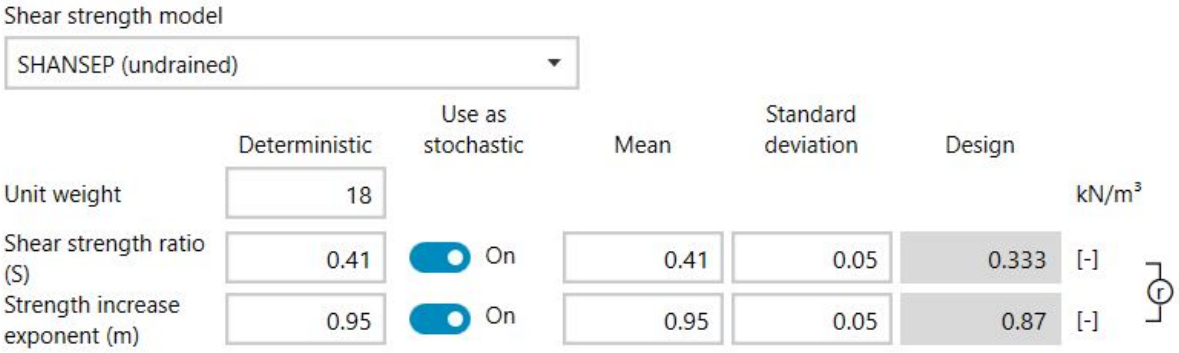

Figure 3.1: Example material parameter input (m and S)

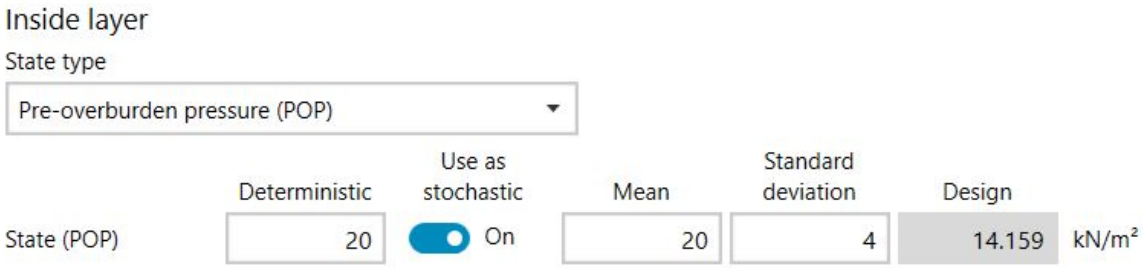

Figure 3.2: Example state parameter input (POP)

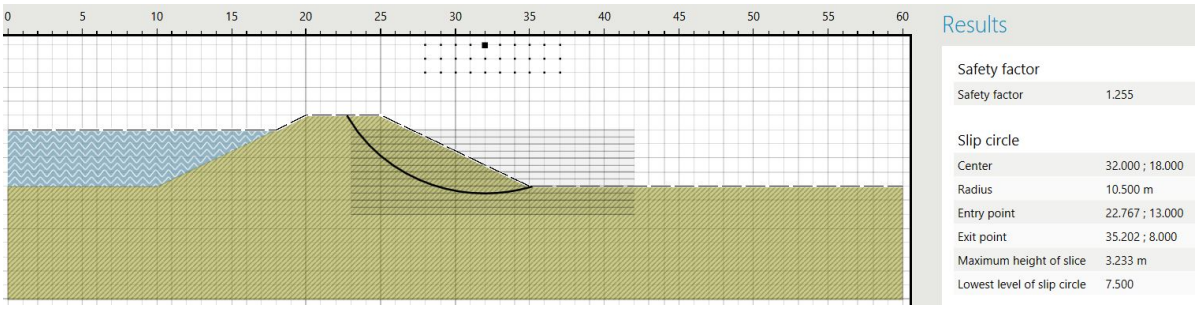

Figure 3.3: Example Bishop calculation result

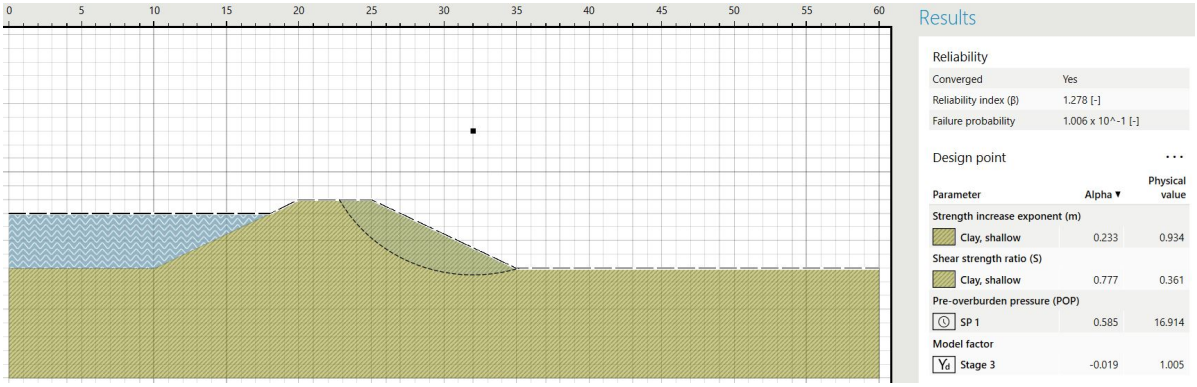

Figure 3.4: Example FORM calculation result

3.1.2. MPM

For a MPM dike stability calculation, a mesh is defined and material points are placed over this mesh. By setting the input parameters, stresses and strains are computed causing the material points to move. The material points start moving trough the mesh until a stable situation is reached or the calculation is stopped. In the final image, the material points have moved throughout the grid and it can be observed whether failure has occurred or not.

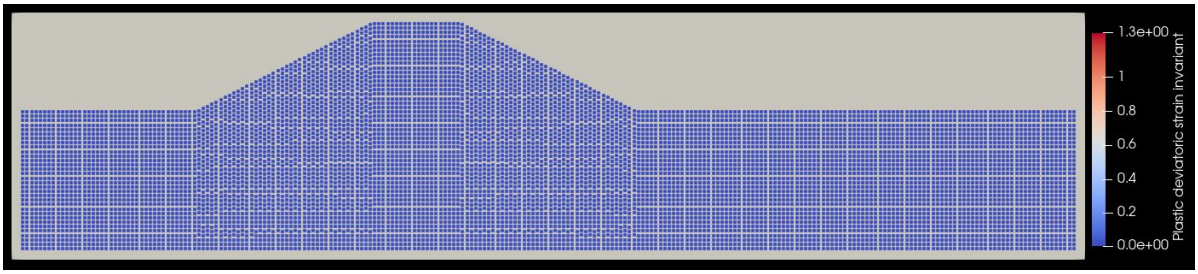

Figure 3.5: Material points in front of mesh before calculation

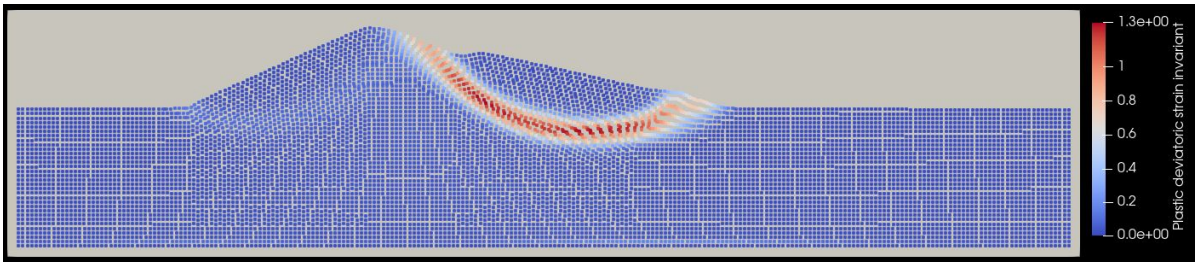

Figure 3.6: Material points in front of mesh after calculation

3.1.3. MPM Failure

For D-Stability failure is straightforward. If the force is greater than the resistance, failure occurs. For MPM however, failure is defined less clearly. For the MPM model, we have to come up with our own failure definition based on how the result of the simulation looks. When the dike fails, sliding occurs over the failure plane. The result of this sliding is that the top of the dike is interrupted by the failure plane and the residual width of the dike is decreased. In Figures 3.7 and 3.8 the difference can be observed. In Figure 3.7, the disturbance in the top of the dike by the slipping of the dike along the failure surface is significantly larger than in Figure 3.8. The failure of the dike is defined by the residual width of the dike. If the residual width of the dike remains intact, it is assumed that failure did not occur. If the residual width of the dike is decreased, it is assumed that failure did occur.

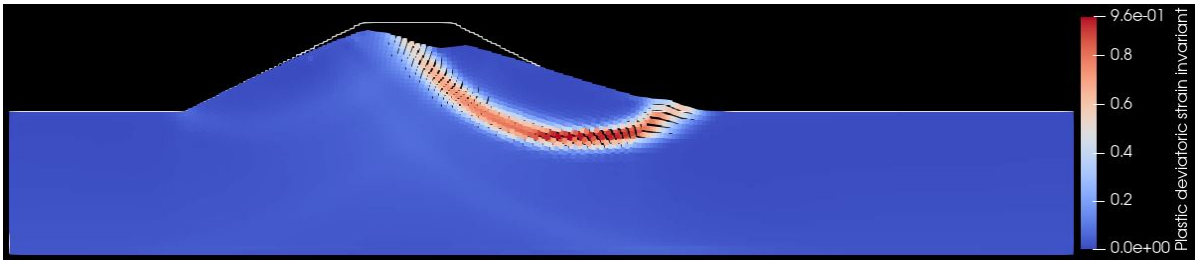

Figure 3.7: Dike failure: dike top interrupted

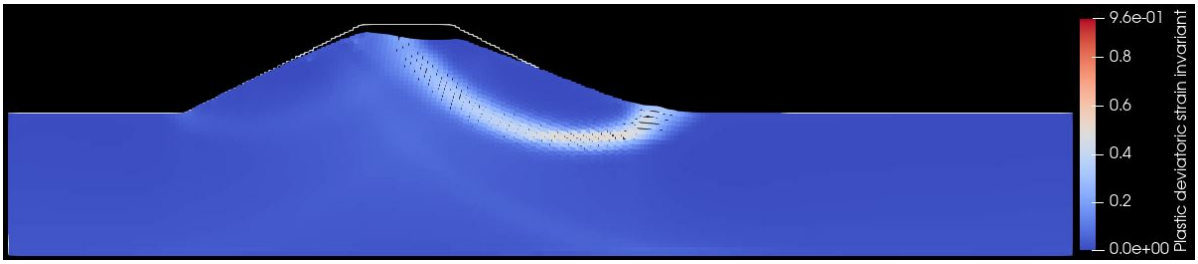

Figure 3.8: No dike failure: dike top still intact

3.2. Proposed Method - Retrogressive Slope Failure

A method is proposed to integrate D-Stability and MPM to estimate the probability of flooding. In 3.2.1, an overview of the method is given with an overview in Figure 3.11. How the method works exactly is explained in Section 3.2.2 and the variations to the method are elaborated in Section 3.3.

3.2.1. Method Overview

This section explains the workings of a method that combines MPM and D-Stability. This combined method has the advantage of a quick probabilistic FORM assessment, coupled with the modelling of the post-failure behavior.

Step 1

The input of the model are the distributions of the SHANSEP parameters, m, S and POP, the dike cross-section and the water level. With these input parameters, a deterministic calculation is performed in D-Stability with the parameter mean values. The result of this calculation is the shape of the critical slip surface and a factor of safety.

Step 2

With the result of this first calculation, a probabilistic FORM analysis can be performed in D-Stability. The probability of failure along the slip surface with the lowest factor of safety is calculated as $P(I_1)$. In D-Stability, the parameter values in the design point, for which failure is most likely to happen, are determined.

Step 3

The dike cross-section is loaded in the MPM-model and a material point distribution is created. The SHANSEP input parameters are the parameter values of the design point calculated in 3.2.1. With the design point values of m, S and POP, the MPM calculation is performed. The result is dike failure along the previously determined slip plane and a residual geometry and a residual dike height. If the residual dike height is lower than the water level, it is assumed that flooding has occurred.

Step 4

If flooding did not occur, the residual geometry of 3.2.1 is now plotted back in D-Stability by transforming the material point grid to a surface line and plotting it in D-Stability. Then the steps are repeated. The material point locations are not taken from the final step in the previous calculation like in Figure 3.9. The material points are redetermined from the surface line to mitigate the effects of large deformations. The new locations of the material points for the dike cross-section are given in Figure 3.10. In Figure 3.10 the overall shear strength is lower. This is because the updated values from the design point are used for the new calculation. The difference between Figure 3.9 and Figure 3.10 is the relocation of the material points. By distortion of the material points in Figure 3.9 a greater distance between the material points causes averaging of the strength parameters, which distorts the results. By redetermining the material point locations, this issue issue is solved.

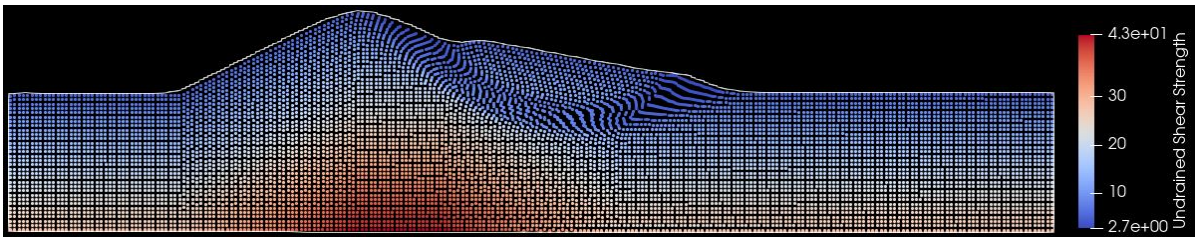

Figure 3.9: MPM calculation 1 final dike undrained shear strength

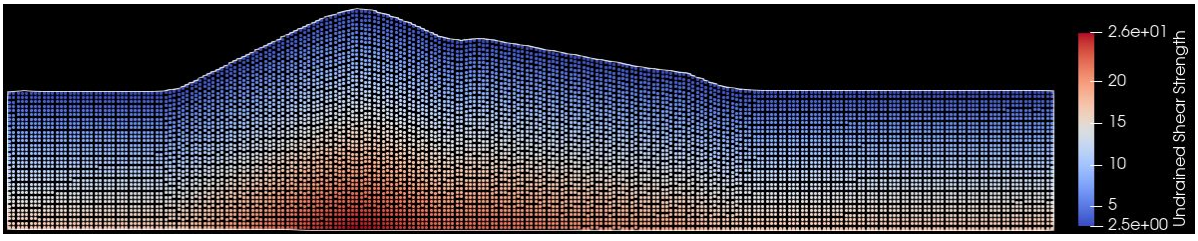

Figure 3.10: MPM calculation 2 initial undrained shear strength

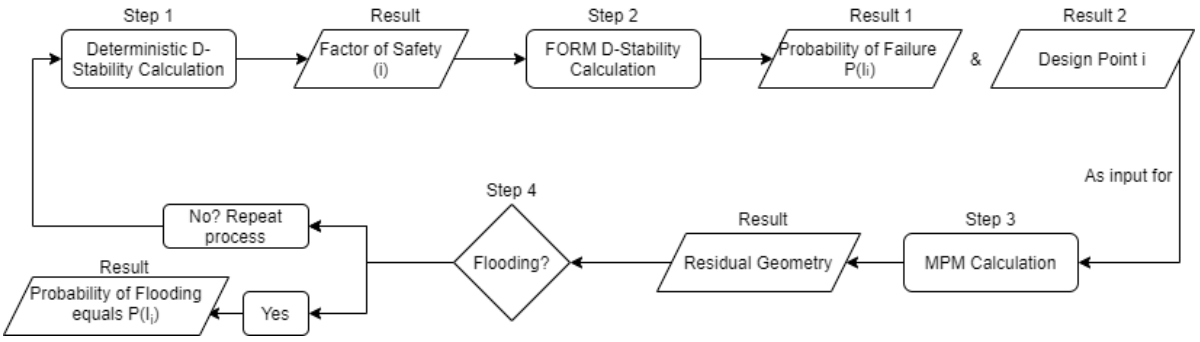

Figure 3.11: Method flow chart

3.2.2. Workings

To connect D-Stability and MPM, the input parameters of both models should be the same. There are however some differences between the models that prevent an easy translation between both models. For D-Stability the soil parameters are for example defined per layer. A layer has certain soil input parameters and along a certain slip surface the strength of the soil is determined. The shape of the layer is determined by a polygon that can be created from scratch. The MPM model does not work with set parameters per layer but per material point. Via the shape op the polygon and the defined number of material points, the locations of the material points are determined and every material point gets assigned some property parameters. These parameters include the location, expressed in an X and a Z value, but also a density and an initial shear strength (SU_0). Especially the initial shear strength is of great importance, since it determines for a large part the stability of the soil. The first part in the connection between D-Stability and MPM, is the implementation of the shear strength model used by D-Stability (the SHANSEP model) in the MPM model.

Next to soil parameters, the MPM model needs other input that needs to be predefined as well. The boundary conditions, the loading conditions, the mesh size and the geometry are all specified in different files with parameters that are MPM and soil model specific.

The way that D-Stability and MPM are connected in this thesis, is by automatization of the generation of the input files. With the same shear strength distribution, D-Stability and MPM should yield the same results. In Chapter 4 the shear strength input parameters are equalized and the MPM model parameters are adjusted to give the same results for the same input in both models.

A Python script has been written to import the polygon constructed in D-Stability into MPM and vice versa. In MPM, the D-Stability polygon can then be converted into a grid of material points by MPM.

Once the material points are generated, the water level and the corresponding water pressures are calculated at all of the material points. Then the stresses are calculated at each point and the pre-overburden pressure is applied at each point. With this information and the SHANSEP input parameters, the SHANSEP undrained shear strength at each material point is computed. With this information, the input files for the MPM calculation can be created again and the MPM computation is started with the same input parameters as D-Stability.

When the calculation is finished, the residual geometry exists of a grid of material points. Via a Python script, this grid is converted into polygon that can be loaded into D-Stability. The water level within the dike should be adjusted to the new geometry of the dike. Then a new D-Stability calculation can be performed and the process is repeated until the water level is lower than the top of the dike.

3.3. Method Variations

There are several applications for the method and their difference lies with the issue of the water level. The method in general calculates for a set water level the probability that flooding occurs. From here three main application methods are proposed: the "Method Retrogressive Flooding by Multiple Water Levels", the "Method Retrogressive Flooding by Critical Water Levels", and the "Method Flooding by Single Instability".

3.3.1. Method 1 - Multiple Water Levels

The method is repeated for several water levels and for each water level the probability of each instability is plotted in a fragility curve. The results are plotted against the water level and the instabilities that lead to flooding are indicated. In the resulting figure, the probabilities of all the instabilities and the probabilities of

flooding at the selected water levels can be seen.

3.3.2. Method 2 - Critical Water levels

The second application of the method is the identification of the **"critical water levels"** for which the probability of flooding is highest after a number of instabilities. A critical water level here indicates the lowest water level for which flooding occurs after a specified number of instabilities.

In Figure 3.12, the original dike cross-section can be observed. In Figure 3.13 it can be seen that for the specified water level after one instability, the dike floods. The critical water level for one instability is therefore determined as 11.75 meter.

The critical water levels for each number of instabilities determined by plotting the successive most likely instabilities for the mean water level of the Gumbel distribution. The result is a residual height after each most likely instability. The residual dike height after a number of instabilities is the critical water level.

This method is more effective than Method 1 since the analysis is only performed for when the probability of flooding is the highest. Less MPM analyses are needed which greatly reduces the computation time.

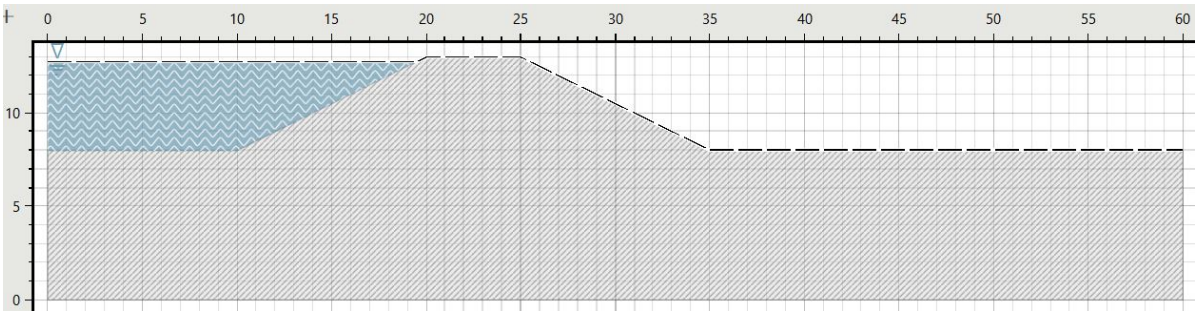

Figure 3.12: Dike cross section with a set water level

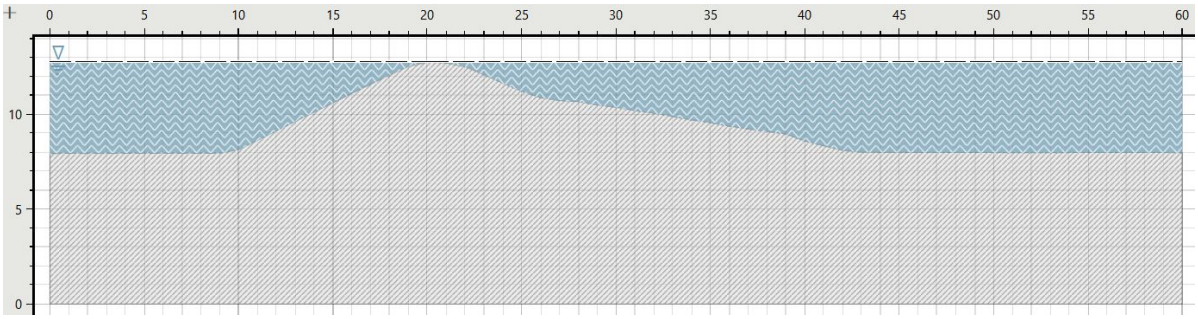

Figure 3.13: Critical water level for the first instability

3.3.3. Method 3 - Flooding by Single Instability

Next to the connection between D-Stability and MPM, a method is proposed to estimate the probability of flooding for a single instability with D-Stability. This method is referred to as **"Flooding by Single Instability"**, or **Method 3**. The method estimates the initial failure surface where flooding just occurs like in Figure 3.14. This is done by increasing the radius of the slip circle for the most likely instability until the slip circle reaches the water body. A D-Stability then a probabilistic analysis is performed over the slip surface and the design point of that calculation is plotted in MPM to check whether flooding does occur. By performing the calculation for multiple water levels, a fragility curve can be made that indicates the water level with the highest probability of flooding.

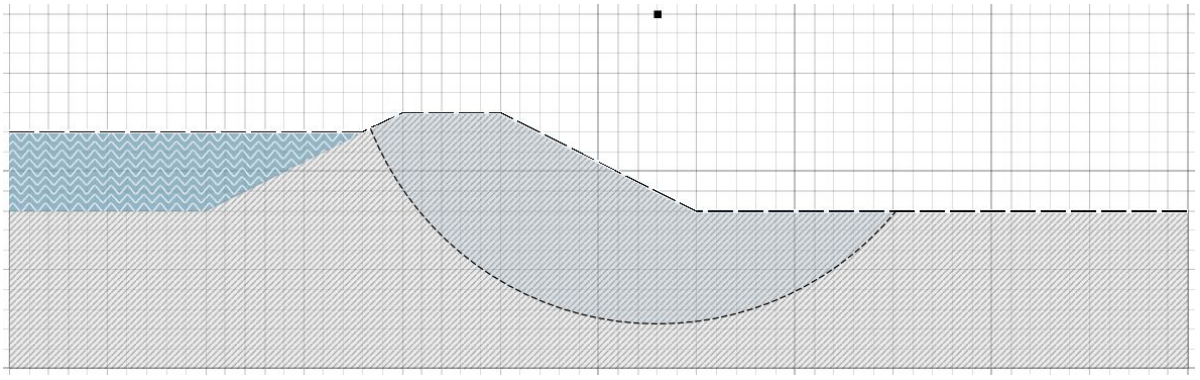

Figure 3.14: Estimation of a single failure plane leading to flooding

- Method 1: Estimate the probability of flooding by retrogressive failure for multiple water levels
- Method 2: Estimate the probability of flooding by retrogressive failure for the critical water levels
- Method 3: Estimate the probability of flooding by a single instability for multiple water levels

3.3.4. Conclusion

A method is proposed to combine D-Stability and the MPM model. The method provides the option to perform a D-Stability calculation and still receive information on the post-failure behavior of the dike. Three distinct applications are proposed which focus on flooding after (1) retrogressive failure for multiple water levels, (2) retrogressive failure at critical water levels, and (3) single instabilities for multiple water levels, respectively.

4

Model Input

The dike stability calculations of the different methods can be qualitatively compared by performing the same scenario calculations for each method. Therefore, the input of both methods should be the same, such that the result should be similar if the methods predict failure behavior accurately. In other words, the calculations should be standardized. This chapter will explain why the selected calculation methods are chosen and how the different parameter values are determined. First the SHANSEP shear strength distribution is applied to MPM. Then the results of both methods are compared in a sensitivity analysis that determines the values for the MPM specific parameters. When the model parameters are determined and the calculations are comparable, the methods are connected to be used complementary

4.1. Standardize Calculations

To standardize the calculations, both methods are compared on a simple deterministic analysis. The cross-section consists of a single homogeneous material. The result of the deterministic calculation in D-Stability is a factor of safety. This factor of safety can be compared with MPM, i.e. in MPM failure should occur for a factor of safety below one, while the dike should be stable for a factor of safety above one.

4.1.1. Cross-Section

To compare the outcomes and potentially find improvements to the calculation methods, first D-Stability and the MPM model need to find similar outcomes to similar calculations. To use both methods supplementary, they are tested by calculating the stability of the same dike. Since the methods use a different calculation method, it is of key importance to equalize the parameters that both models use and know what these parameters are. A clay of which such properties are known is the clay used in Van der Krogt et al. (2019). The dike used by Van der Krogt et al., (2019) consists of two clay layers and a sand layer. The clay from the dike core in this cross-section is selected as a representative clay. The data retrieved in this section will be mainly from Van der Krogt et al. (2019). A cross-section of the dike can be found in Figure 4.1

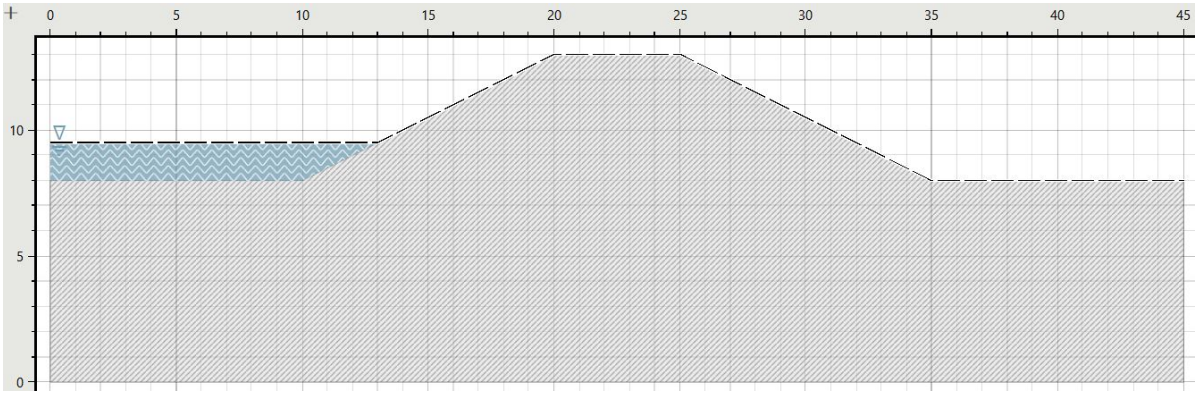

Figure 4.1: Reference dike example cross-section

4.1.2. Undrained Shear Strength

The reference dike is a clay body and this means the most influential factor on the dike stability is the undrained shear strength (SU) of the material. MPM and D-stability used different constitutive models, Von Mises and SHANSEP respectively, to evaluate the strength of the material. The Von Mises constitutive model uses a shear strength value uncorrelated from the effective stresses in the material. A plastic strain softening model is used in MPM, such that during plastic deformation, the shear strength reduces from a peak shear strength to a residual shear strength. The user can specify different undrained shear strength values for larger sections of material points to incorporate previous stress effects or model different clay layers, and a depth trend may be included in the shear strength.

D-Stability uses a different approach to determine the shear strength in the soil. D-Stability uses the SHANSEP model to determine the initial shear strength distribution of the clay within the dike based on the stress and stress history of the material. For the SHANSEP model, the initial shear strength distribution is a function of the strength, stress and stress history of the soil, whereas the MPM model uses a predefined initial shear strength distribution.

This discrepancy in shear strength distributions makes combining both methods difficult. Therefore, the model parameters would need to be converted from one model to the other in order to standardize the calculations. Between the MPM and the D-Stability models, as indicated, the key difference is situated in the determination of the initial shear strength distribution. To address this problem, the shear strength values of the SHANSEP model are transferred to the material points of the MPM model, and used as the undrained shear strength of the Von Mises constitutive model. By transferring these initial shear strengths, both models should perform the same calculation on the same dike and both models will have the same (SHANSEP) input parameters with their corresponding distributions.

Next to the initial undrained shear strength (SU_0), MPM uses a peak and residual undrained shear strength (SU_{Peak} and SU_{Res}). Part of the sensitivity analysis is to determine the SU_{Peak} and SU_{Res} values. The peak and residual shear strengths are here assumed to be factors of the imported SHANSEP initial shear strength. The peak shear strength is considered to be equal to the initial shear strength (factor equals 1) and the residual shear strength is considered to be half the peak shear strength (factor equals 0.5).

4.2. MPM Setup

For the standardization of both calculation models, it is imperative to correctly determine the input parameters. There are more input parameters for the MPM model than for the D-Stability model. This discrepancy means that a division is made between parameters that are used by both models and parameters that are only used by the MPM model. The parameters that the MPM model uses, but that are not used by D-Stability in the calculations, are considered fixed in all calculations, i.e. no variability is applied to these properties. These parameters will further be referred to as MPM parameters. The parameters that are used by both models are in turn referred to as D-Stability Input Parameters as they eventually are varied in the probabilistic calculations.

For the MPM model there are more input parameters that are used to calculate the stresses in the soil that are not varied. During the Sensitivity Analysis one of the goals is to determine the value of these parameters so that D-Stability and MPM can be correctly compared by varying the material properties.

MPM Input Parameter	**Mean (μ)**	**Unit**
Residual Factor (r_f)	0.5	kN/m^2
Peak Factor (p_f)	1.0	kN/m^2
Hardening Modulus (H_h)	1000	kN/m^2
Softening Modulus (H_s)	-9.5	kN/m^2
Young's Modulus (E)	3000	kN/m^2
Poisson's Ratio (v)	0.31	[-]
Density (e)	1.8	kg/m^3

Table 4.1: Example MPM input parameters - determined via sensitivity analysis

D-Stability Input Parameter	Mean (μ)	Std. Deviation (σ)	Char. Value	Unit
Unit Weight (γ)	18	-	-	kN/m^3
Shear Strength Ratio (S)	0.36	0.012	0.34	[-]
Strength Increase Exponent (m)	0.98	0.006	0.97	[-]
Pre-Overburden Pressure	20	4	x	kPa

Table 4.2: D-Stability Input Parameters

$$\tau = SU_0 = \sigma'_v \times S \times \frac{\sigma'_y}{\sigma'_v}^m \tag{4.1}$$

The SHANSEP undrained shear strength is transferred to the material points by first exporting the surface line from D-Stability to a Python. A grid of material points is created based on the D-Stability surface line of the dike cross-section and defines a water level. The stresses are then calculated over the grid, based on the density of the water and the soil, from which the SHANSEP shear strength of each material point is calculated with Equation 4.1. The resulting output is a grid with the distribution of the initial shear strength calculated by the SHANSEP model over the dike cross-section as given in Figure 4.2, which can be used as input in MPM.

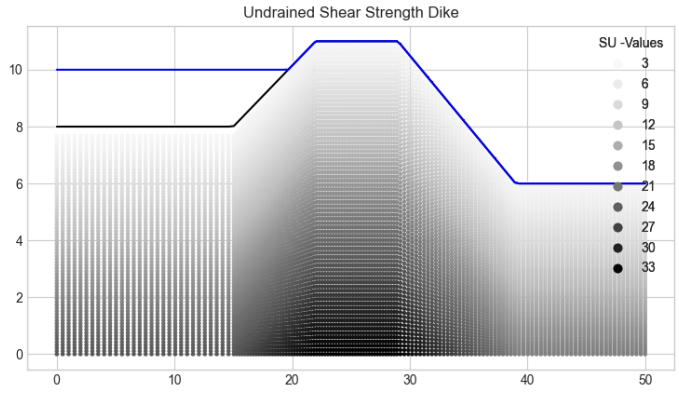

Figure 4.2: SU distribution in dike

4.3. Sensitivity Analysis

Now that D-Stability Input Parameters are standardized, the MPM parameters should be determined. The MPM Input parameters are determined by means of a sensitivity analysis. The aim of the sensitivity analysis is determining for which MPM Input Parameters both models fail with the same D-Stability Input Parameters.

The first MPM Input Parameter that will be looked at is the stiffness of the dike. The MPM model uses the Young's Modulus (E) of the clay to determine the elastic stress-strain behaviour of the soil. From USACE (1990), several representative values for the stiffness of clay soils were found. It is expected that the factor of safety for the different stiffness values is equal, but that the post-failure behaviour of the dike differs per stiffness.

Soil Type	Characteristic Value	Unit
Very Low Stiffness Clay	480 - 4,800	kPa
Low Stiffness Clay	4,800 - 19,000	kPa
Medium Stiff Clay	19,000 - 48,000	kPa
Stiff Clay	48,000 - 95,000	kPa

Table 4.3: Characteristic Stiffness Values (USACE, 1990)

Next to the Young's Modulus, the sensitivity of the peak and residual factors, p_f and r_f, is investigated. By default the residual factor (r_f) is set to 0.5. This means that the soil can lose up to 50 percent of its shear strength when it fails. This behaviour is associated with soil softening and is a result of the softening of the soil and the build-up of pore water pressures in the soil. As pore water pressures are not yet incorporated within the model, the decrease in shear strength associated with pore pressure build-up is incorporated in the r_f term.

As hardening is not considered for the dikes investigated here, the peak factor (p_f) is said to be equal to one. This also means that the soil hardening gradient (H_h) is of no influence since the soil does not harden. Both the peak factor and the soil hardening parameter are therefore left out of the sensitivity analysis.

The factor corresponding to the r_f term, is the soil softening modulus (H_s). This term indicates the plastic strain needed to reach the residual strength (Wang, 2017). The process of soil softening is visualized in Figure 4.3. The softening parameter has a negative value and determines for a large part what failure looks like when it happens. By increasing the gradient, converging it to zero, the soil will lose its shear strength more quickly and thus failure happens more instantaneous. If the parameter is decreased, the soil reaches its residual shear strength over more time, altering the failure process.

By default, the soil softening parameter (H_s), has a set value that is constant throughout the dike. However, it is also possible to use a constant residual plastic strain ($\bar{\epsilon}_r^p$). This means that the softening parameter varies throughout the dike while the required plastic strain to reach the residual strength is constant. The relation between the residual plastic strain and the soil softening modulus is given in equation 4.2 (Wang, 2017).

$$\bar{\epsilon}_r^p = \frac{r_f c_0 - c_0}{H_s} = \frac{(r_f - 1)c_0}{H_s} \tag{4.2}$$

The results of the sensitivity analysis will be compared with dike calculations from D-Stability. It will be tested whether the dikes with a factor of safety above one are indeed stable, and that dikes with a factor of safety below one indeed fail. The failure planes of the dikes that fail will then eventually assessed on their shape based on literature on dike failure.

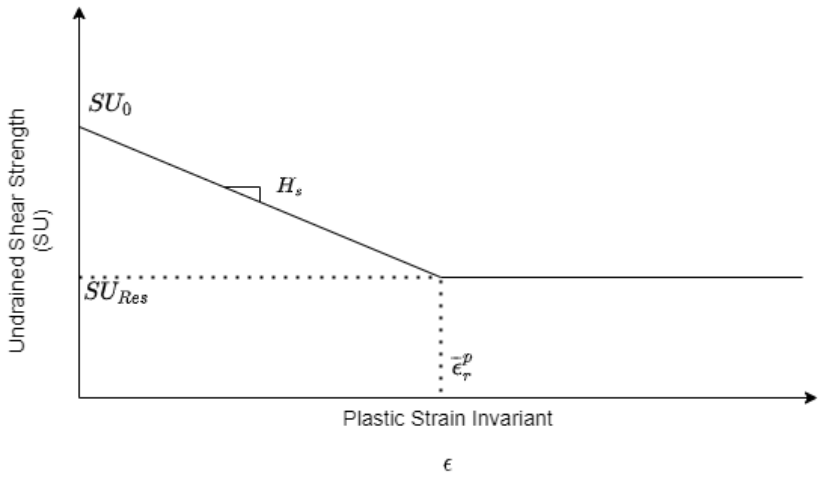

Figure 4.3: Softening modulus (H) in cohesion softening model (Wang, 2017)

4.3.1. D-Stability Calculations

The first calculation that is performed is a deterministic Bishop slip surface calculation in D-Stability. In this case, the reference dike is as defined in Sections 4.2 and is used by Van der Krogt et al. (2019). The dike is visible in Figure 4.1. The initial input parameters are given in Table 4.4 and result in a Bishop calculation in D-Stability with a factor of safety of exactly 1.0. As the factor of safety is exactly at failure, it is possible to determine when failure exactly occurs in the MPM model.To compare this to a situation where failure does not occur (the factor of safety is above one), the pre-overburden pressure (POP) is slightly increased. This gives a factor of safety of slightly above one.

Two cases with a slightly different POP value have been selected to pinpoint the moment of failure. The dike case that leads to failure is called Dike 1 and the dike case that remains stable is called Dike 2. The D-Stability results of both dike cases can be found in Figures 4.4 and 4.5. Dike 1 and Dike 2 have safety factors of respectively 1.0 and 1.011. This means that failure should occur in the MPM model for the dike in Figure 4.4 and failure should not occur for the dike in Figure 4.5.

Input Parameter	**Dike 1**	**Dike 2**	**Unit**
Unit Weight (γ)	18	18	kN/m^3
Shear Strength Ratio (S)	0.36	0.36	[-]
Strength Increase Exponent (m)	0.98	0.98	[-]
Pre-Overburden Pressure	15.6	16	kPa
Water Level Left	10	10	m
Factor of Safety	1.0	1.011	[-]

Table 4.4: D-Stability unstable (1) and stable (2) input parameters

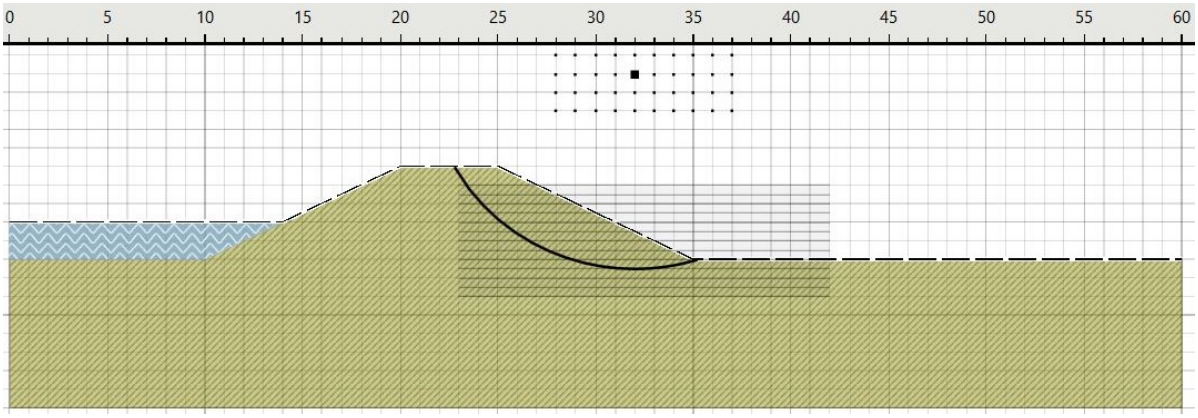

Figure 4.4: Bishop failure plane dike 1: POP = 15.6

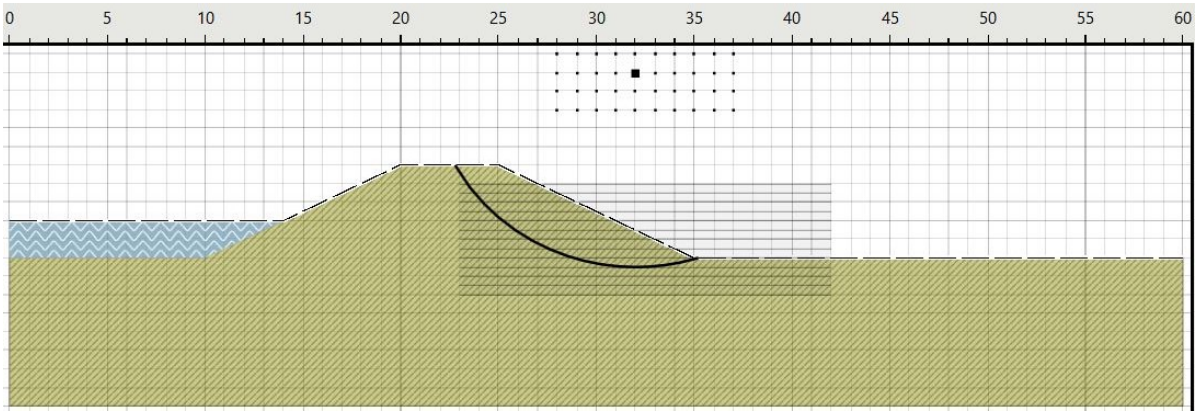

Figure 4.5: Bishop failure plane dike 2: POP = 16

4.3.2. MPM Calculations

Whereas the calculations in D-Stability provide a straightforward answer to whether failure occurs, failure is a bit harder to determine in the MPM calculations. Especially with lower elasticity values, some displacements within the dike occur without this leading to failure. It is therefore useful to determine a clear failure definition at the margins of dike failure.

The general definition for failure in an MPM analysis comes down to the presence of a sliding plane. This is a shear band region with increase plastic deviatoric strain, and a large displacement of the dike along this shear band region. The result of the shearing plane is a discontinuity in the top of the dike. The residual width of the top of the dike decreases as failure happens, but remains constant as failure does not yet occur.

The difference between failure and non-failure can be seen in Figures 4.6 and 4.7. Whereas Dike 1 has a large displacement along the region with the large plastic deviatoric strain, Dike 2 shows significantly less displacement along the shear region. The top of Dike 2 is still intact: failure did not occur.

For dikes with a lower elasticity it is harder to determine the exact moment of failure. With lower instabilities, dike failure

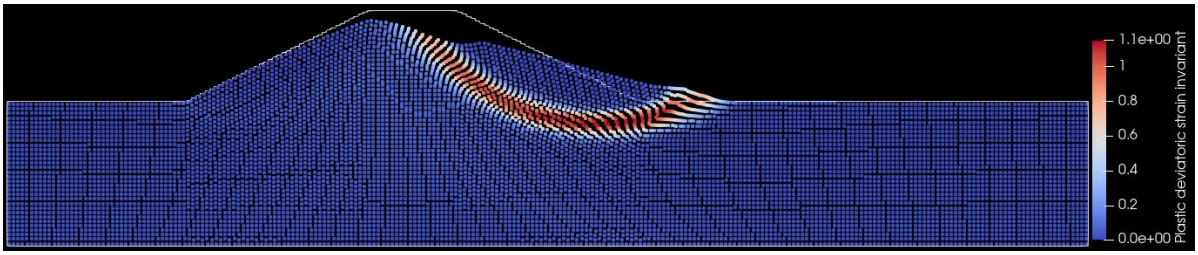

Figure 4.6: Dike 1: failure occurs

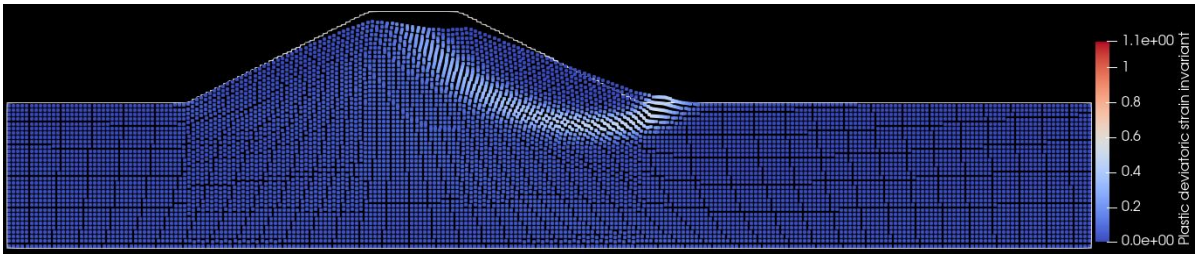

Figure 4.7: Dike 2: failure does not occur

4.3.3. Optimum Input Parameters

From the definition of failure given in 4.3.2, the optimum MPM input parameters from Table 4.1 can be determined. From D-Stability, the input parameters at the moment of failure are known. Now the MPM results should be equalized to the D-Stability results. The best results for the MPM analysis are obtained when the softening modulus is set to -9.5 when a constant softening modulus is used or when the residual plastic strain is set to 0.65. For these input values the dike fails when the factor of safety is determined to be 1.0 by D-Stability and is stable when the factor of safety is higher than one. The input values form Table 4.4 are used for the dike case where the factor of safety is one, and the the pre-overburden pressure is increased to sixteen kPa to simulate a stable dike. The optimum parameters can be found in Table 4.5. The cross-section images of the performed analysis that yielded the results can be found in Appendix A.

Input Parameter	**Value**	**Unit**
Residual Factor (R_f)	0.5	[-]
Softening Modulus (H_s)	-9.5	kN/m^3
Residual Plastic Strain ($\bar{\epsilon}_r^p$)	0.65	kN/m^3

Table 4.5: Fixed Input Parameters

4.3.4. Time

An important factor in the MPM calculations is time. To know whether failure has taken place and what it looks like, the calculation should be carried out long enough for the failure to indeed take place. When the

calculation is ended too soon, failure might not yet have happened. Too long calculations are however neither desired since they take longer.

If failure occurs, it mostly occurs within the first five seconds of the calculation. For this report the standard calculation time is fifteen seconds. This is deemed enough time for any failure to have occurred. Especially around the margin, so with a factor of safety of around one and with low values of elasticity, it appeared form analyses that this time is needed. The lower value for the elasticity leads to less instantaneous failure, as the elastic deformations take place before failure happens.

The calculation can however also be stopped when either no movement occurs anymore. This is recommended for Monte Carlo analyses to save time for calculations for which no failure occurs.

4.3.5. Mesh Size Sensitivity

Mesh size has a significant importance on the quality of the calculations but also on the time of the calculations. Because of parameter averaging, the MPM results with the same input for a coarse mesh will indicate a stronger dike than expected. With the smallest mesh size set to 0.5 meter and the number of material points per element direction set as two for both directions, acceptable results are found.

A way of determining whether the mesh size results are acceptable, is via the Young's Modulus. Different values for the elasticity of the dike give different strength results for a coarse mesh while this is not to be expected. If the results of the analysis are the same for different values of elasticity, the results of the analysis are deemed correct. Although the results were similar for higher Young's Modulus values, the high elasticity caused for the unexpected movement of material points due to an error in MPM for higher elasticity values.

It can be investigated whether there is a relation between the strength parameter of the dike and the coarseness of the mesh. If such a relationship exists, the input parameters can be adjusted to the mesh size, speeding up the calculations. This can be verified by using a finer mesh.

4.3.6. Conclusion

After incorporating the SHANSEP shear strength parameters into the MPM model, the best results are found when using a constant residual plastic strain ($\bar{\epsilon}_r^p$) of 0.65 or a Softening Modulus (H_S) of -9.5 and a corresponding residual factor (R_f) of 0.5. When using these input parameters, the Young's Modulus has little to no effect on the size and shape of the failure plane and changing it led to unexpected results caused by a MPM error.

Time is of importance for the model, the calculation time is set to fifteen seconds to make sure that every possible dike failure took place.

The mesh size is important. The results for a coarse mesh were not satisfactory. Henceforth a relatively fine mesh is selected at the cost of time. If a relationship can be constructed between the mesh size and the strength parameters in the dike, this poses a potential time saving solution to the long calculation time of a fine meshed analysis.

Overall the SHANSEP parameters serve as a useful input to the Material Point Method model. The results of the MPM calculations are comparable to the D-Stability calculations.

The next chapter will use the determined parameters as input for the proposed method and tests the method.

5

Combining Methods: The Probability of Flooding

This chapter develops a method to improve the calculation of retrogressive slope failure using D-Stability and the material point method. The proposed method is exemplified in a reference case study. The results are compared with conventional methods, MPM, RMPM and D-Stability.

5.1. Introduction

Now that the input parameters are determined and both methods perform the same calculation, the newly proposed method for the determination of dike stability can be tested and compared with current methods. The aim of the method is estimating the probability that flooding of the dike will occur as accurate as possible without it costing too much time. Via a case study, the method will be put into practice. The results of the cases study will then later be verified by means of a RMPM analysis in Chapter 6.

First, the method and the different variation are briefly recapped. Then, the practical use of the method and its different variations are demonstrated by means of a case studies. When the practical use of the method is clarified, the practical application and the results of different types of analyses are discussed.

5.2. Proposed Method - Recap

This section recaps how the method works and then how the method is applied. In Figure 5.1, a schematic overview of the method is visible. In Section 5.3 the method is performed for a single water level to clarify the practical use of the method. A more detailed description of the individual steps of the method can be found in 3.2.1.

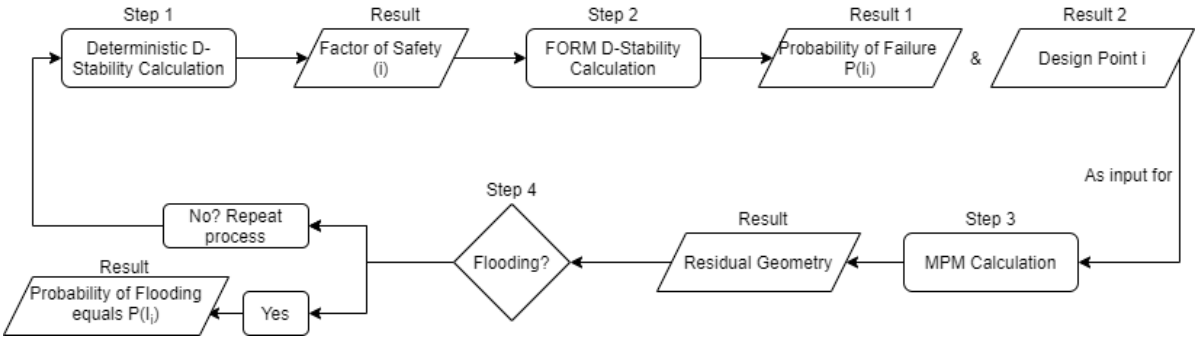

Figure 5.1: Method flow chart

5.2.1. Multiple Water Levels - Method 1

By combining D-Stability and MPM, the probability of flooding by retrogressive slope failure for a given water level can be determined. However, since the water level is not constant, multiple analyses should be conducted for multiple water levels to get a better image of the overall stability of the dike. From the analyses

performed at different water levels, fragility curves can be constructed that plot the probability of the successive instabilities versus the water level. In Section 5.4 the method is performed on different water levels.

5.2.2. Critical Water Levels - Method 2

Doing multiple analyses at multiple water levels is however quite time consuming. To save time, the analysis is conducted over several water levels where the probability of flooding is expected to be the highest. The principle on which this is based is that the probability of flooding is highest if the water level of the dike is just higher than the residual height of the dike.

In Section 5.5 first the critical water levels are identified. At these water levels, the probability of flooding after a number of instabilities is expected to be the highest. Then the method is performed for these water levels to determine the probability of flooding for these set water levels.

5.2.3. Flooding by Single Instability - Method 3

Next to flooding by retrogressive slope failure, flooding can also occur after one instability. Via D-Stability, a method is created to approximate the flooding probability after one instability for a given water level. The results of this approximation are later tested in a full RMPM Monte Carlo analysis.

5.3. Fixed Water Level Worked Example

With the new method the probability of flooding can be calculated for a set water level. An example of the method is presented below. The D-Stability input parameters can be found in Table 5.1. The MPM input parameters are the values determined by the sensitivity analysis in Section 4.3.3. The water level in this example is conditional to a water level of 11.75 meter. From Equation 2.19 this water level yields to a probability of $1.89 \cdot 10^{-5}$ for a water level of 11.75 meter.

Variable Input Parameter	**Mean (μ)**	**Std. Deviation (σ)**	**Unit**
Unit Weight (γ)	18	-	kN/m^3
Shear Strength Ratio (S)	0.41	0.05	[-]
Strength Increase Exponent (m)	0.95	0.05	[-]
Pre-Overburden Pressure	10	4	kPa

Table 5.1: Dike input parameters

Gumbel Parameter	μ	β	**Unit**
Water Level Distribution	9.6	0.17	m
	Water Level	**Probability**	**Unit**
Water Level Probability	11.75	$1.89 \cdot 10^{-5}$	m

Table 5.2: Dike input parameters

5.3.1. First Instability

The reference dike that has the parameters given in Table 5.5 yields the results visible in Figure 5.2 and Table 5.3. The most likely failure plane is determined by D-Stability to be the failure plane visible in Figure 5.2, and the corresponding factor of safety and failure probability are given in Table 5.3.

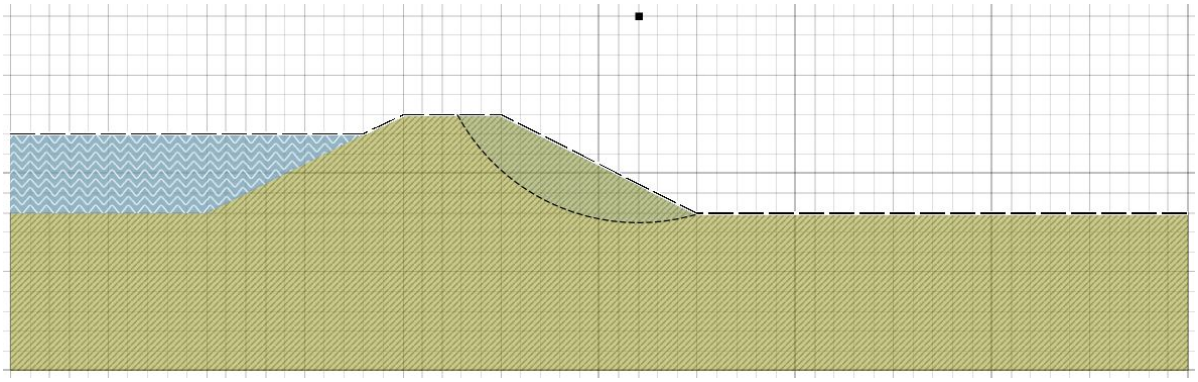

Figure 5.2: D-Stability Bishop calculation

Factor of Safety	**0.932**	[−]
Probability of Failure $P(I_1)$	$7.22 \cdot 10^{-1}$	[−]
Reliability Index β	-0.589	[−]
Design Point:	-	[−]
Strength Increase Exponent (m)	0.953	[−]
Shear Strength Ratio (S)	0.426	[−]
Pre-Overburden Pressure	11.018	kPa

Table 5.3: D-Stability calculation result

The design point from Table 5.3 is then used as input for MPM. The residual dike height determined by the MPM calculation is **12.74 meter**. This means the top of the dike has decreased 26 centimeters in height by the first instability according to MPM. The MPM result can be seen in Figure 5.3

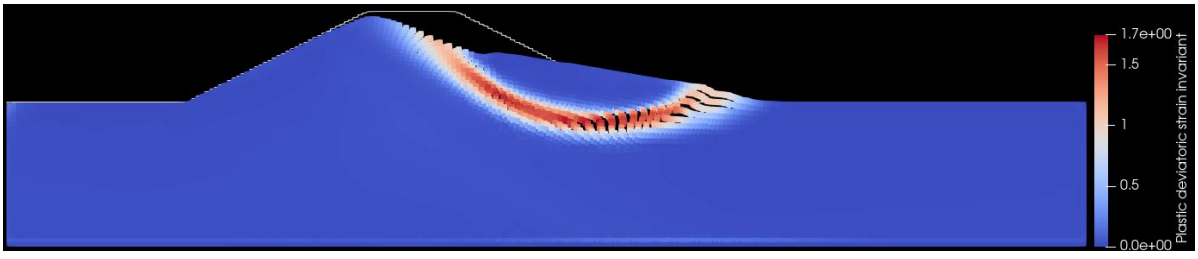

Figure 5.3: MPM result of the first instability

5.3.2. Calculation of the Second Instability

Since flooding does not yet occur, the process is repeated. The residual geometry from Figure 5.3 is loaded back into D-Stability, which gives Figures 5.4 and 5.5. The results of the calculation are presented in Table 5.4. In the table it is shown that the most critical slip surface is situated on the outward side of the dike by a narrow margin of $8 \cdot 10^{-}5$.

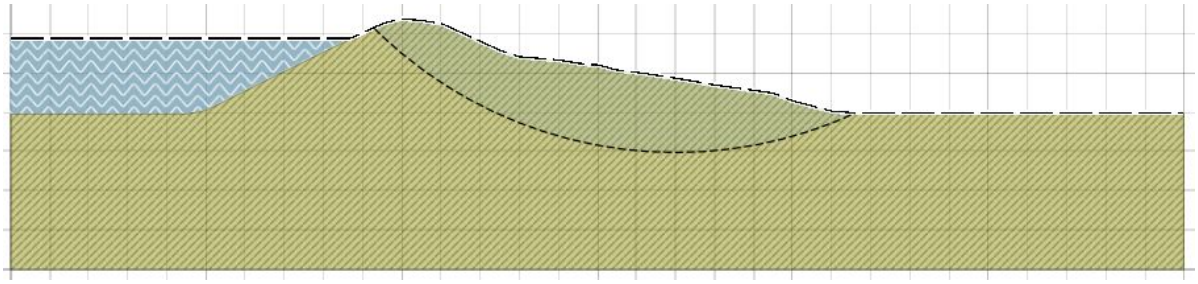

Figure 5.4: D-Stability FORM probability calculation

Figure 5.5: D-Stability FORM probability calculation outward

[-]	**Inward Dike**	**Outward Dike**	**Unit**
Factor of Safety	1.617	1.686	[-]
Probability of Failure $P(I_1)$	$1.361 \cdot 10^{-3}$	$1.369 \cdot 10^{-3}$	[−]
Reliability Index β	2.998	2.996	[−]
Design Point:	-	-	[−]
Strength Increase Exponent (m)	0.937	0.935	[−]
Shear Strength Ratio (S)	0.297	0.302	[−]
Pre-Overburden Pressure	5.278	4.826	kPa

Table 5.4: D-Stability FORM calculation results

The new MPM calculation result with the failure plane on the right side of the dike as predicted by D-Stability is given in Figure 5.6. The maximum dike height of the MPM result **11.6 meter** and thus lower than the water level of 11.75m. This is visualized in Figure 5.7. As seen in Figure 5.6, failure appears to have occurred on the inward side of the dike. This can be explained by the narrow margin between the probabilities of failure on the inward and outward side of the dike from Table 5.4. D-Stability and MPM yield the same results up to a certain degree, apparently failure in MPM occurs slightly before failure in D-Stability.

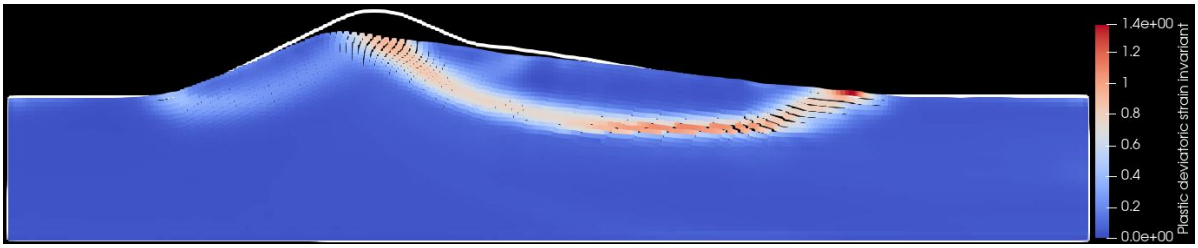

Figure 5.6: MPM calculation 2 plastic deviatoric strain invariant

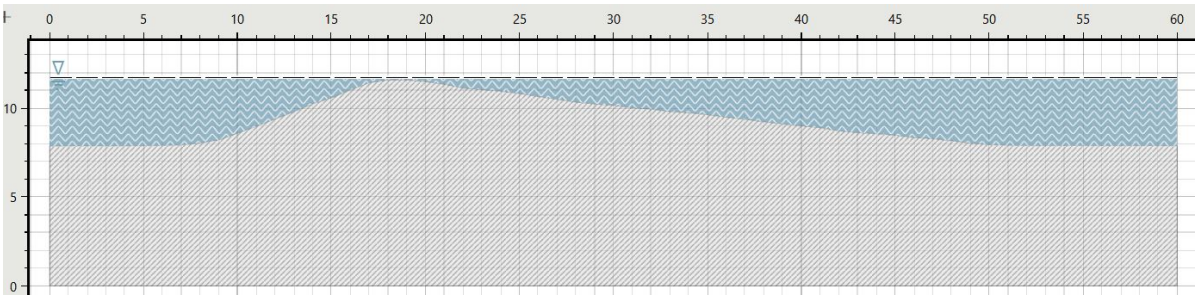

Figure 5.7: Residual geometry versus water level in D-Stability

In Figure 5.6 it can be observed that failure happened on the inside dike. This can be explained by the small difference between the probability of failure on inward dike and failure on the outward dike. The sensitivity analysis of Chapter 4 was not accurate enough for this order of difference.

5.3.3. Results - Method Single Water Level

According to the proposed method, flooding happens after two instabilities have occurred. If both instabilities are fully dependent, the probability of flooding is equal to the probability of the smallest instability occurring, this is a conservative estimate (Van der Krogt et al., 2019) and (Van Montfoort, 2018). In the case of the example, with fully dependent failure planes, the probability of failure that leads to flooding for a water level of 11.75 meter, would be equal to the probability of the second instability, which is $1.361 \cdot 10^{-}3$. In this probability the probability of a water level of 11.75 meter occurring is not yet incorporated. By Van der Krogt et al. (2019), the probability of flooding, taking into account the water level, is given by equation 5.1.

$$P(F) = \int P(F|h) f(h) dh \tag{5.1}$$

The probability of a water level of 11.75 meter occurring is in Table 5.2 determined as $1.89 \cdot 10^{-5}$. The probability of flooding conditional to the water level then becomes $2.572 \cdot 10^{-8}$, which corresponds to a reliability index of 5.45.

5.4. Flooding by Retrogressive Failure: Multiple Water Levels - Method 1

An example distribution of the input parameters is taken from Van der Krogt et al. (2019) and are given in Table 5.5. The difference in the parameter distributions with the previous example, given in Table 5.1, is an increase in the Pre-Overburden Pressure, the result of this is a higher factor of safety for the dike and henceforth a lower probability of flooding.

Variable Input Parameter	**Mean (μ)**	**Std. Deviation (σ)**	**Unit**
Unit Weight (γ)	18	-	kN/m^3
Shear Strength Ratio (S)	0.41	0.05	[-]
Strength Increase Exponent (m)	0.95	0.05	[-]
Pre-Overburden Pressure	20	4	kPa

Table 5.5: Dike input parameters

5.4.1. Method 1 - Results

From these input parameters it can be calculated for different water levels what the probability of flooding is as a result of retrogressive slope failure.

In Table 5.7 and Figures 5.8 and 5.9, it can be observed that two scenarios of retrogressive slope failure lead to flooding. For a water level of eleven meters the dike floods after three instabilities. For a water level of twelve meter the dike floods after two instabilities. To then calculate the probability of flooding conditional to the water level Equation 5.1 is used. In Table 5.8 it can be seen that for the two cases that lead to flooding, the reliability indices conditional to the water level are respectively 7.452 and 7.1. The probability of flooding is largest for a water level of twelve meters after two instabilities.

There may however be a water level where the probability of flooding is higher for a water level somewhere between the currently selected water levels. With every extra instability, the probability of flooding decreases significantly as seen in Table 5.7. Therefore Method 2 aims to calculate the highest probability of flooding after a number of instabilities. This way the highest probability of flooding can be determined.

Also the computation time of Method 1 is rather long. In order to make Figure 5.8, thirteen MPM analyses of each about twenty minutes of computation time had to be made. These analyses are time consuming and although thirteen analyses is still significantly less then the thousands of analyses need for a RMPM Monte Carlo analysis, it is desired to decrease this number of analyses even more, which is why Method 2 is proposed.

Water Level	**Probability**	**Reliability Index (β)**
9 m	1	7.196
10 m	0.509	$-2.158 \cdot 10^{-2}$
11 m	$1.559 \cdot 10^{-3}$	2.956
12 m	$4.348 \cdot 10^{-6}$	4.473

Table 5.6: Dike input parameters

WL	$P(I_1)$	**FL?**	$P(I_2)$	**FL?**	$P(I_3)$	**FL?**	$P(I_4)$	**FL?**
9 m	$1.006 \cdot 10^{-1}$	**No**	$9.131 \cdot 10^{-3}$	**No**	$9.984 \cdot 10^{-9}$	**No**	$1.401 \cdot 10^{-15}$	**No**
β	1.278	-	2.36	-	5.612	-	7.899	-
10 m	$1.006 \cdot 10^{-1}$	**No**	$7.285 \cdot 10^{-4}$	**No**	$2.152 \cdot 10^{-9}$	**No**	$8.78 \cdot 10^{-16}$	**No**
β	1.278	-	3.183	-	5.872	-	6.558	-
11 m	$1.006 \cdot 10^{-1}$	**No**	$1.387 \cdot 10^{-5}$	**No**	$2.943 \cdot 10^{-11}$	**Yes**	-	-
β	1.278	-	4.191	-	6.547	-	-	-
12 m	$1.006 \cdot 10^{-1}$	**No**	$1.47 \cdot 10^{-7}$	**Yes**	-	-	-	-
β	1.278	-	5.127	-	-	-	-	-

Table 5.7: Retrogressive slope failure results (FL? indicates if flooding occurs)

Water Level (m)	$P(h)$	$P(I_{Flooding})$	**Reliability Index Flooding β**
11	$1.559 \cdot 10^{-3}$	$2.943 \cdot 10^{-11}$	7.452
12	$1.41 \cdot 10^{-5}$	$1.47 \cdot 10^{-7}$	7.1

Table 5.8: Reliability index flooding for Method 1

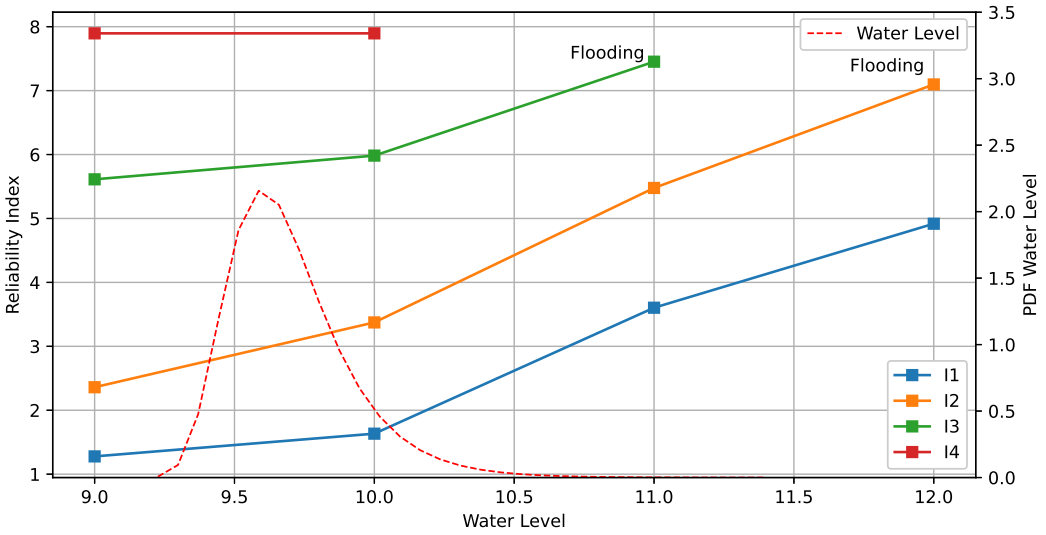

Figure 5.8: Fragility curve fully dependent - water level probability incorporated

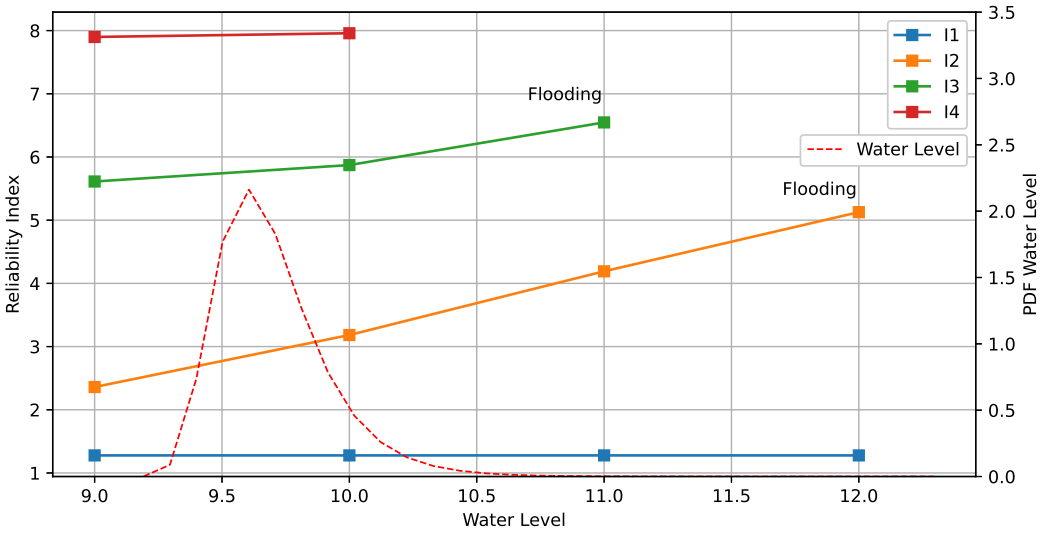

Figure 5.9: Fragility curve fully dependent - water level probability not incorporated

5.5. Critical Retrogressive Flooding - Method 2

The most critical situation by retrogressive flooding occurs if the water level is just higher than the dike after a number of instabilities. By plotting the residual dike height after multiple instabilities by transferring the geometry from D-Stability to MPM and vice versa, an image can be created on what the residual dike geometry will be after a number of instabilities. By doing this for four different water levels, Figure 5.10 is created. In the figure it can be observed that flooding occurs after two instabilities for a water level of twelve meter and after three instabilities for a water level of eleven meters. It can however be seen that the residual dike height after a number instabilities is relatively independent of the water level.

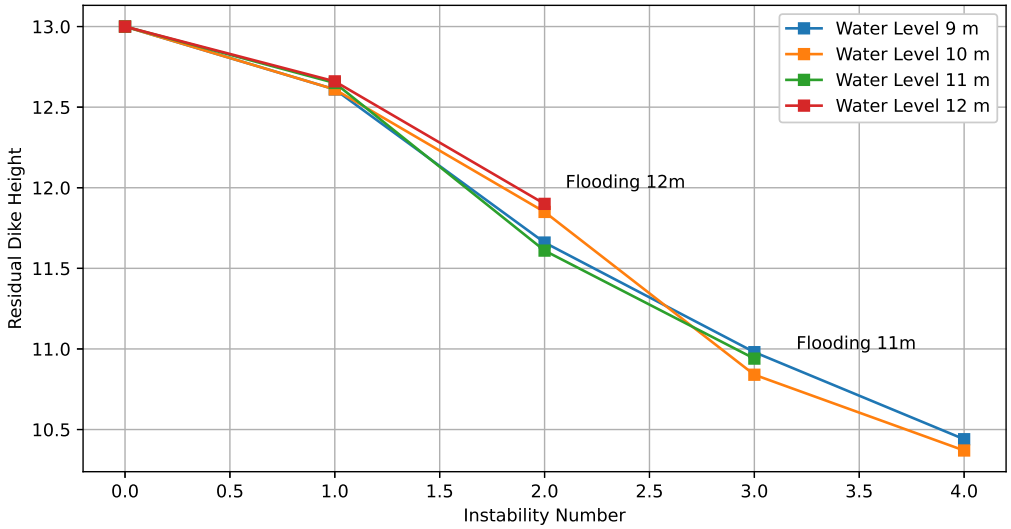

Figure 5.10: Residual dike height after a number of instabilities

If the residual dike height is estimated per instability, the most critical situations for retrogressive slope can be assessed. In the case presented, the most critical water level after two instabilities is around 11.8 meter. For three instabilities it appears that the critical water level is around eleven meter. For a water level of eleven meter, the probability of flooding is already determined to be smaller for retrogressive slope failure than for a single instability leading to failure.

5.5.1. Method 2 - Results

The failure probabilities for the critical water levels after one, two and three instabilities are given in Table 5.5. Conditional to the water level, the probabilities of flooding are presented in Table 5.10. The highest probability of flooding by retrogressive failure is by two successive instabilities and a water level of 11.8 meter.

The analysis for Method 2 first requires the determination of the critical water levels. This is done by performing the method on the mean water level. After four instabilities it was determined that flooding cannot realistically occur for the mean water level. The determination of the critical water levels took four MPM calculations. The analysis was then repeated for the critical water levels for flooding after two and three instabilities. In total, this brings the amount of MPM analyses to nine. Counting fifteen minutes per MPM analysis, Method 2 takes about three hours.

WL	$P(I_1)$	**Flooding?**	$P(I_2)$	**Flooding?**	$P(I_3)$	**Flooding?**
11	$1.006 \cdot 10^{-1}$	**No**	$1.387 \cdot 10^{-5}$	**No**	$2.943 \cdot 10^{-11}$	**Yes**
β	1.278	-	4.191	-	6.547	-
11.8	$1.006 \cdot 10^{-1}$	**No**	$1.742 \cdot 10^{-7}$	**Yes**	-	-
β	1.278	-	5.095	-	-	-

Table 5.9: Critical retrogressive slope failure

Water Level (m)	$P(h)$	$P(I_{Flooding})$	**Reliability Index Flooding β**
11	$1.559 \cdot 10^{-3}$	$2.943 \cdot 10^{-11}$	7.452
11.8	$1.41 \cdot 10^{-5}$	$1.742 \cdot 10^{-7}$	6.908

Table 5.10: Reliability index flooding for one instability

5.6. Flooding by Single Instability - Method 3

By setting constraints for the failure plane in D-Stability, the probability of a slip plane that leads directly to flooding occurring can be estimated. As seen in Figures 5.11 and 5.12, the estimation of the single failure plane can be approximated quite accurately by increasing the radius of the most likely slip surface to just reach the water level. The results can be found in Table 5.11.

The estimation of the failure plane leading to flooding is repeated for several water levels. By incorporating the water level probability in the flooding probability results, the water level with the highest probability of flooding can be determined. The results of this analysis can be found in Table 5.12.

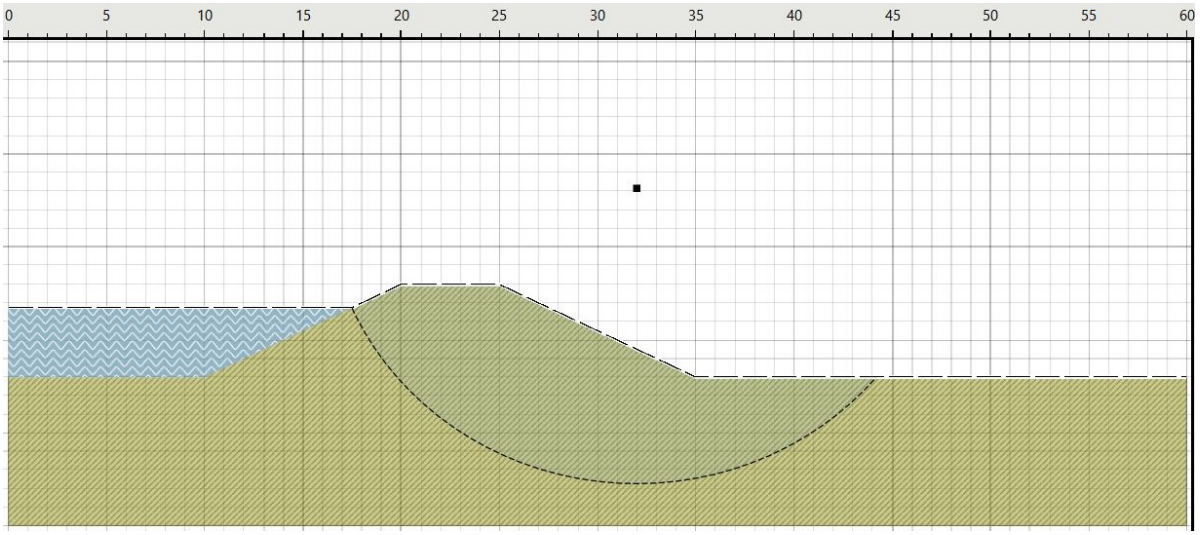

Figure 5.11: Slip surface that leads to flooding after one instability

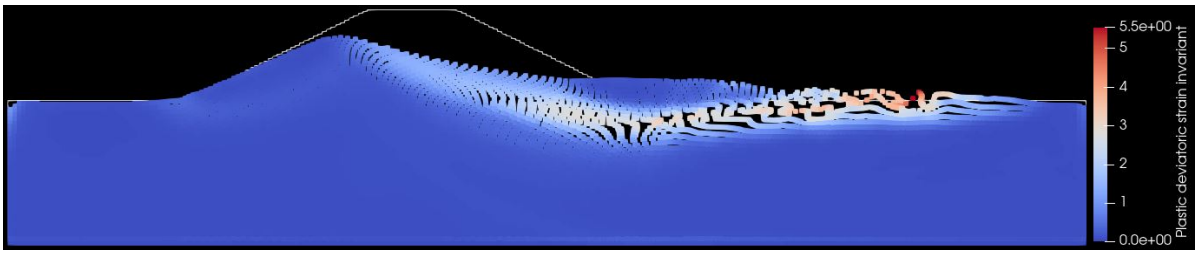

Figure 5.12: Slip surface that leads to flooding after one instability MPM

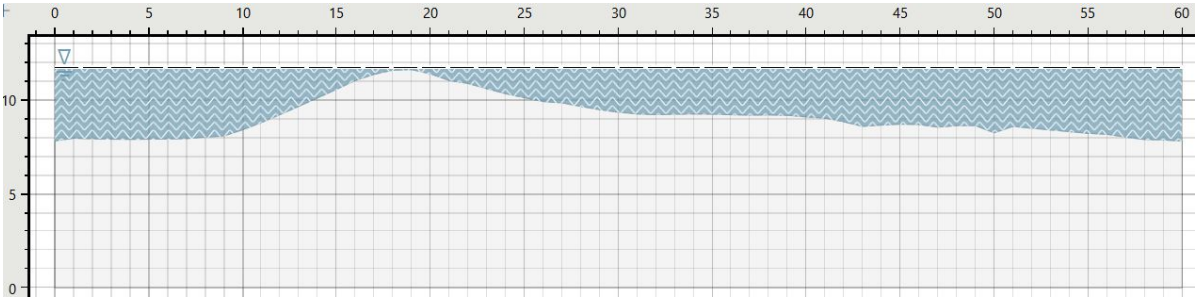

Figure 5.13: Water level higher than the residual dike height

Factor of Safety	**1.73**	[−]
Probability of Failure $P(I_1)$	$5.189 \cdot 10^{-3}$	[−]
Reliability Index β	2.563	[−]
Design Point:	-	[−]
Strength Increase Exponent (m)	0.942	[−]
Shear Strength Ratio (S)	0.305	[−]
Pre-Overburden Pressure	6.482	kPa

Table 5.11: D-Stability calculation result - Single instability failure

5.6.1. Method 3 - Results

Additionally, to determine the most critical flooding situation, the probability of a single instability leading to flooding plotted against multiple water levels is plotted in a fragility curve. From this curve the most critical situation for a single instability leading to flooding is visualized in Figure 5.14. For a single instability flooding is most likely to occur for a water level of 12 meter.

This analysis required seven MPM runs. This amounts to a total computation time of about two and a half hours.

Water Level (m)	$P(h)$	$P(I_1)$	**Reliability Index Flooding** β
9.5	1.75	$2.559 \cdot 10^{-17}$	7.824
10	0.509	$1.213 \cdot 10^{-13}$	7.413
10.5	$2.939 \cdot 10^{-2}$	$1.407 \cdot 10^{-10}$	6.834
11	$1.559 \cdot 10^{-3}$	$4.721 \cdot 10^{-8}$	6.408
11.5	$8.235 \cdot 10^{-5}$	$5.119 \cdot 10^{-6}$	6.137
12.0	$4.348 \cdot 10^{-6}$	$1.929 \cdot 10^{-4}$	6.026
12.5	$2.296 \cdot 10^{-7}$	$2.764 \cdot 10^{-3}$	6.071

Table 5.12: Reliability index flooding for one instability

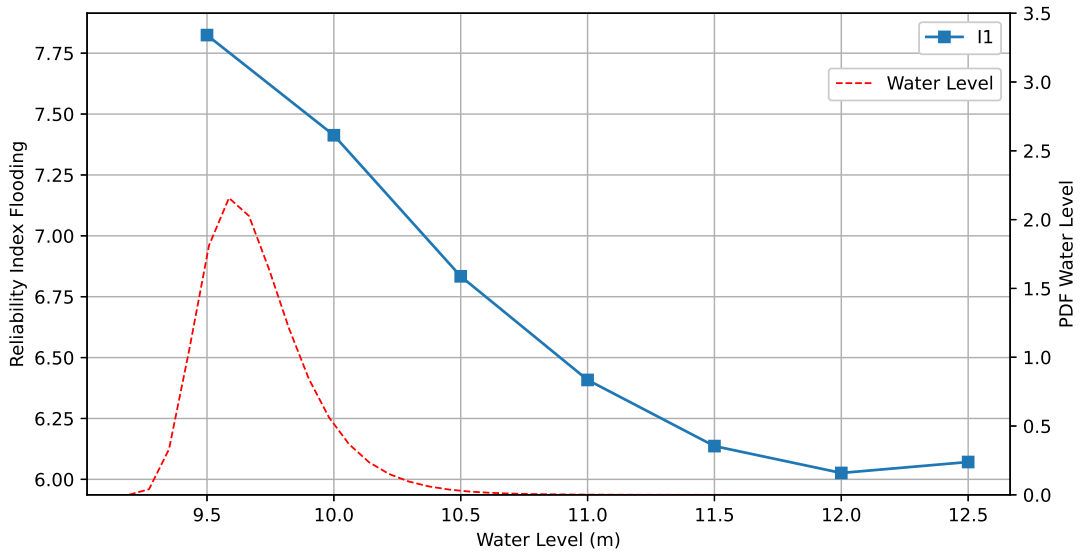

Figure 5.14: Fragility curve single instability that leads to flooding

5.7. Conclusion

The Material Point Method and the D-Stability limit equilibrium method can be used complementary to predict when failure will happen and what it will look like. This offers the possibility to look at retrogressive slope failure as a critical flooding mechanism.

By Method one, highest probability of flooding occurred for a water level of 12 meters with a reliability index of 7.1. By Method 2 the highest probability of flooding occurred for a water level of 11.8 meters and the reliability index was 6.908. By Method 3 the highest probability of flooding occurred for a single instability at a water level of 12 meters with a reliability index of 6.026. Flooding is most likely to occur by a single failure mechanism for water level of 12 meters.

Although flooding by retrogressive slope failure is not the most likely cause of flooding for the given examples, it could be the critical flooding mode for other dike cross sections with different failure planes. By using the Material Point Method to model the post failure behaviour of the most likely successive instabilities, the most critical situations for retrogressive slope failure can be assessed. The combination between D-Stability and MPM can be used to accurately model the most critical situations for retrogressive slope failure that lead to flooding.

A disadvantage of the proposed method is the time it takes to conduct a MPM analysis. If the time of an MPM calculation can be reduced, for example by adjusting the shear strength parameters, the method promises to be a quick assessment for the risk of flooding by retrogressive slope failure.

Another disadvantage of the proposed method is the complexity of the analysis. The method as it is currently is user-unfriendly and requires a thorough understanding of the different method components. practically it is not easily applicable yet.

In the next chapter, the results of the different analyses will be compared to a full RMPM Monte Carlo Analysis.

6

Random Material Point Method Monte Carlo Verification

6.1. Introduction

By combining D-Stability and the MPM model in Chapter 5, estimations of the probability of flooding and failure of the dike are made. To verify the estimated flooding probability, we compare the results with a RMPM Monte Carlo analysis. The results of both calculations can then be compared to see whether the estimation of the proposed method is similar to the RMPM results.

6.2. RMPM Input Parameters

The most credible probability of flooding comes from a Monte Carlo simulation of the Random Material Point Method. A RMPM Monte Carlo analysis takes into account the parameter variations, models the post failure behavior and can incorporate the soil heterogeneity by applying horizontal and vertical correlation. In this model the shear strength is randomly distributed throughout the dike and correlated vertically and horizontally by means of anisotropy. The condition for modeling the anisotropy is that the horizontal and vertical correlation are known. The results of a RMPM Monte Carlo analysis are a probability of flooding, a probability of failure and the option to view the failure planes of the flooding cases.

6.2.1. Shear Strength Distribution

Important to model this heterogeneity, is the distribution of shear strengths within the dike. As the shear strength in the SHANSEP model is stress dependent, the shear strength distribution is different throughout the dike as it is dependent on the effective stress. For the shear strength distribution in RMPM, this means that throughout the dike, every material point has its own shear strength distribution. The shear strength distributions at the material points are determined by the distributions of the SHANSEP input parameters m, S and POP. The distributions for the specific example are given by Table 6.1. By varying these input parameters at every material point, the corresponding shear strength distributions at the material points can be calculated. in Figure 6.1 example distributions of shear strength values at different depths are given. From the distributions of Table 6.1, 100,000 points are randomly distributed and the corresponding shear strength distributions are determined.

Variable Input Parameter	**Mean (μ)**	**Std. Deviation (σ)**	**Unit**
Unit Weight (γ)	18	-	kN/m^3
Shear Strength Ratio (S)	0.41	0.05	[-]
Strength Increase Exponent (m)	0.95	0.05	[-]
Pre-Overburden Pressure	10	4	kPa

Table 6.1: Clay dike parameter distribution

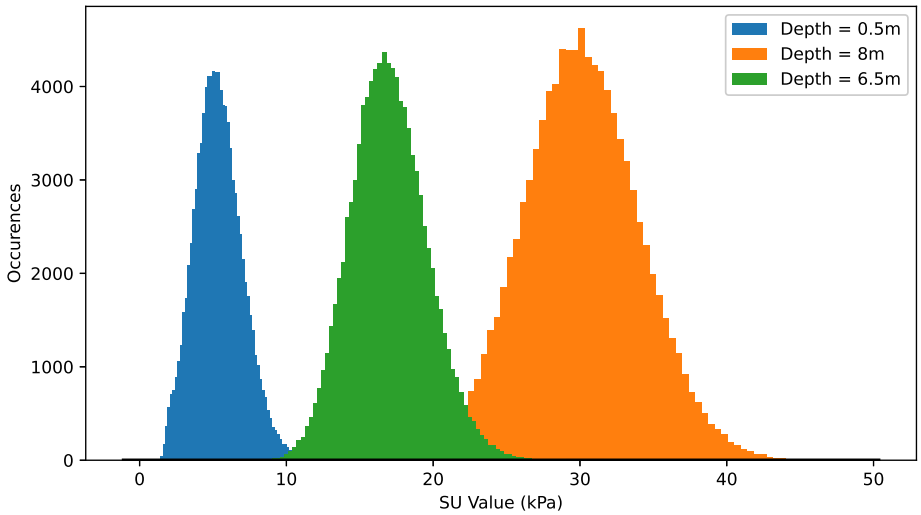

Figure 6.1: Undrained shear strength distributions at different locations (N = 100,000)

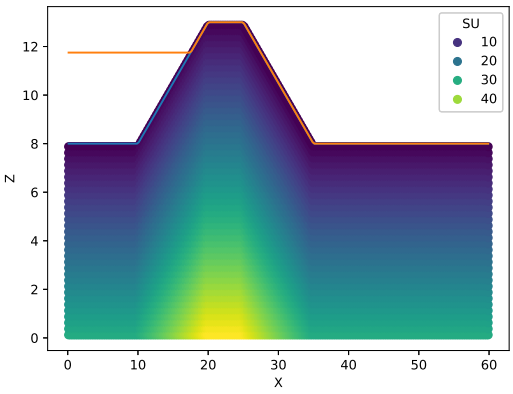

(a) Mean shear strength at the material points

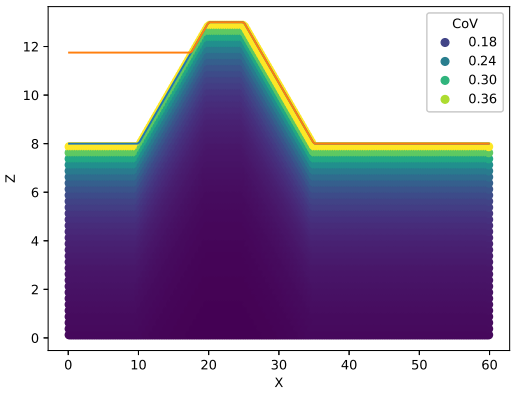

(b) Shear strength coefficient of variation at material points

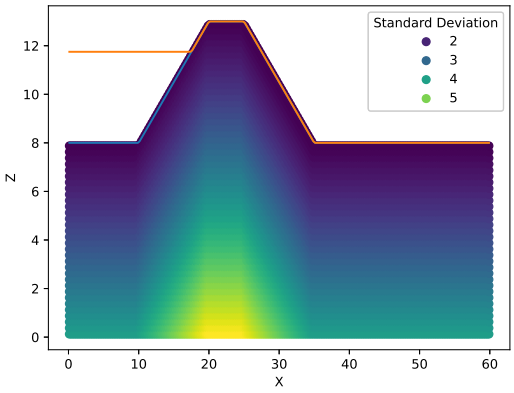

(c) Shear strength standard deviation at material points

Figure 6.2: Shear strength distributions at material point N = 10,000

6.2.2. Random Soil Fields

The shear strength distribution within the dike is the governing input for the shear strength of the dike. However, since it is a soil a degree of heterogeneity exists (Elkateb et al., 2003). This means that the soil has areas that are generally strong and areas that are generally weak. It is however not known where the strong and weak areas exactly are. To mimic this soil characteristic, a lot of different options are plotted in so-called random fields where weak and strong soil areas are altered. To create the random fields and mimic soil heterogeneity, a term is introduced that indicates how large the strong and weak areas generally are: anisotropy. Anisotropy is the correlation of soil areas with similar parameters. A low value for the anisotropy means that weak and strong layers will alternate more often. A high value for the anisotropy means that there is less variation between the parameters in large areas. For this model, the vertical anisotropy is set as one meter and the horizontal anisotropy is set at ten meters. An example of the resulting shear strength distribution in a random field can be found in Figure 6.3.

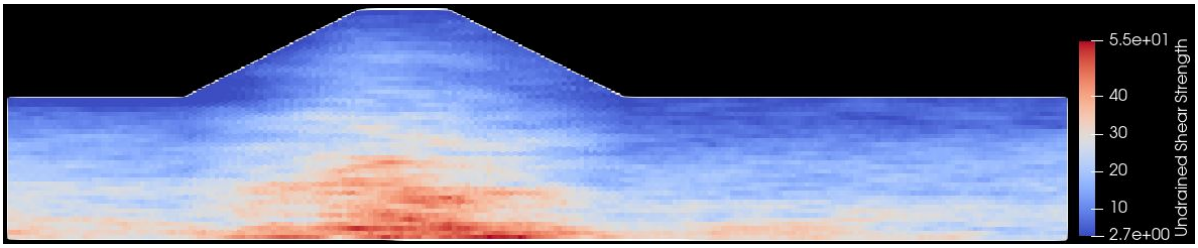

Figure 6.3: Example of the SU distribution in a random field

6.2.3. Residual Plastic Strain

In Chapter 4, the optimum value for the residual plastic strain ($\bar{\epsilon}_r^p$) was determined to be 0.65. For this analysis, a plastic deviatoric strain values of 0.58 and 0.6 were used. These values were used before a redefinition of failure in the MPM model was made. The lower value for the residual plastic strain in the analysis means that more cases will lead to failure than predicted. In the analysis with a residual plastic strain set as 0.58, more cases lead to flooding than in the analysis where the residual plastic strain is set as 0.6. For an analysis with a residual plastic strain of 0.65, flooding is expected to occur in even less cases. The reason the analysis with a residual plastic strain of 0.65 is not performed is practical, as the analysis takes a long time and the added value for this thesis would only be marginally.

6.2.4. Prediction Method: Single Water Level

From 5, the most critical probability of flooding was determined to occur by a single instability. For this analysis, the probability of flooding is conditional to a water level of 11.75 meter. This means that, as taken from Section 5.4, that the probability of flooding is $5.189 * 10^{-3}$ for a single instability, as can be seen in Table 6.2 Figure 6.5. In Section 5.3.3 the probability of flooding by retrogressive failure is determined to be $1.361 * 10^{-3}$. This means that when flooding by a single instability and retrogressive flooding considered to be fully independent, the probabilities of flooding are added to make a total probability of flooding of $6.55 * 10^{-3}$. If both types of flooding are fully dependent, the largest probability is the probability of flooding, which is $5.189 * 10^{-3}$. The true probability of flooding is situated between $5.189 * 10^{-3}$ and $6.55 * 10^{-3}$. The prediction is that flooding occurs roughly every one of 193 simulations.

The probability of dike failure occurring is higher than the probability of flooding. The probability of failure is determined by D-Stability as $7.22 * 10^{-1}$ as can be seen in Table 6.2 and Figure 6.4. This means that it is expected that one in every 1.39 calculations will lead to failure. However, the Random Material Point Method takes into account the heterogeneity of the soil. This means that weak layers and strong layers will alternate each other. This causes for averaging of the soil parameters. For the case study, the dike is generally weak as the factor of safety for a deterministic calculation with mean soil parameters is below one. This means that, with the averaging of soil parameters by the dike heterogeneity, failure is expected to occur more than predicted by the homogeneous D-Stability calculation. The implication this has on the prediction is that more failure cases are predicted by RMPM than by D-Stability.

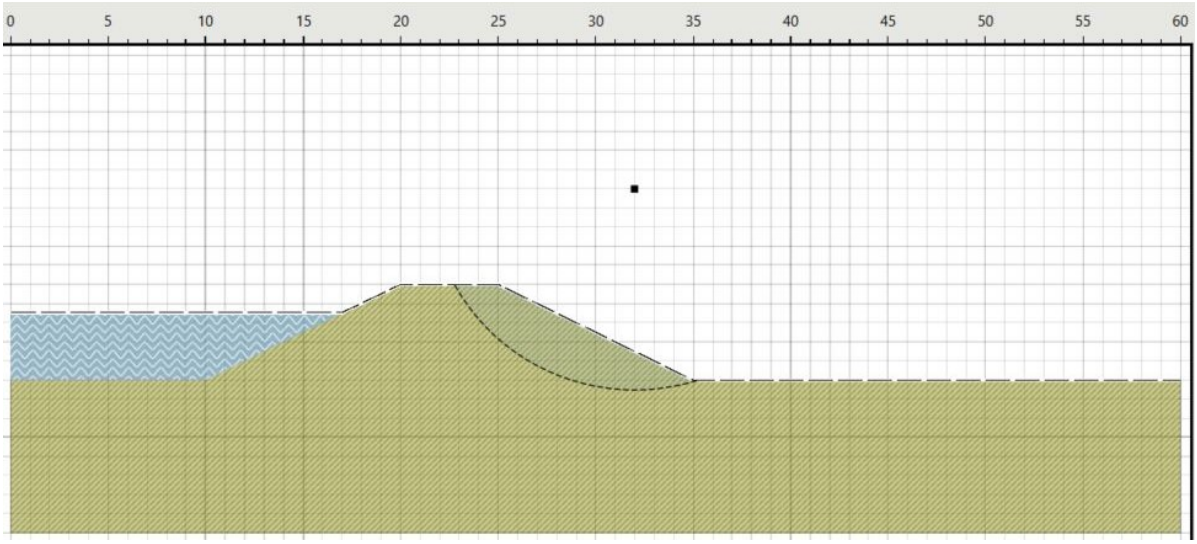

Figure 6.4: D-Stability most likely slip plane

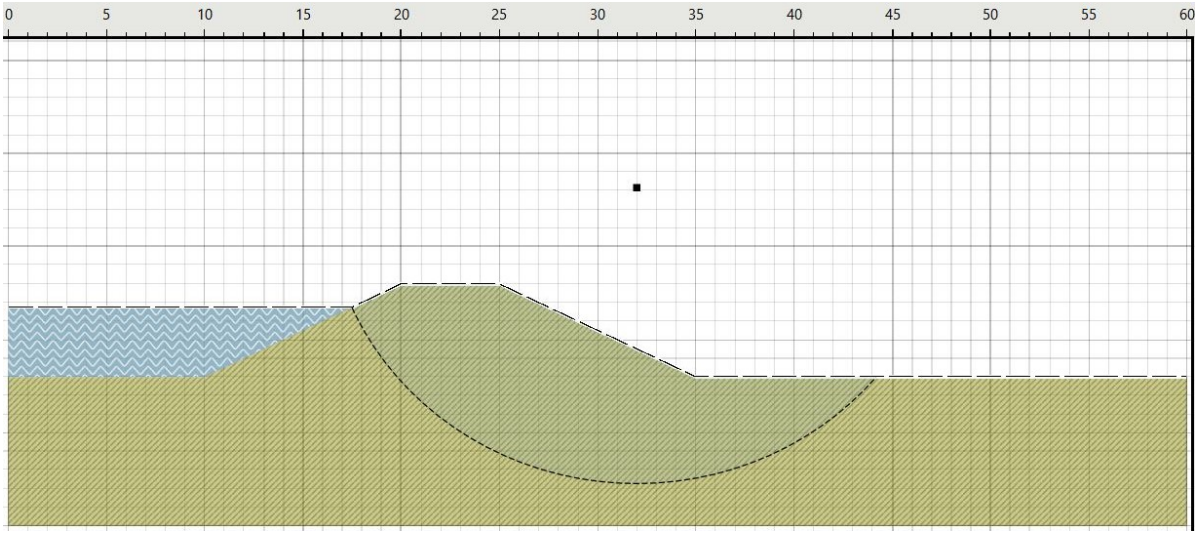

Figure 6.5: Slip plane that leads to flooding after one instability

[-]	**Most Likely Slip Plane**	**Flooding slip plane**	**Unit**
Probability of Failure $P(I_1)$	$7.22 \cdot 10^{-1}$	$5.189 \cdot 10^{-3}$	[−]
Reliability Index β	−0.589	2.563	[−]
Design Point:	-	-	[−]
Strength Increase Exponent (m)	0.953	0.942	[−]
Shear Strength Ratio (S)	0.426	0.305	[−]
Pre-Overburden Pressure	11.018	6.482	kPa

Table 6.2: D-Stability FORM calculation results

6.3. RMPM Results - Flooding Probability

After the determination of the input, the analysis can be performed. From the data first the probabilities of flooding and failure are determined. Afterwards the individual failure cases that lead to floods will be investigated to see what type of failure leads to flooding.

6.3.1. Flooding Probability

By the estimation that flooding is likely to occur for one in every 193 simulations, the number of simulations is set to 10,000. This means that it is expected that around 52 cases will lead to flooding. As mentioned in 6.2.4, since soil heterogeneity is not taken into account in the prediction by the method, the number of floods is expected to be lower by RMPM than by the prediction of the proposed method. The effect of soil heterogeneity in the RMPM simulation is however expected to be partially cancelled out by the reduced value of the residual plastic strain ($\bar{\epsilon}_r^p$).

Constraints are placed to determine what calculations lead to flooding and what calculations lead to failure. For flooding the constraint is straightforward: If the residual dike height is smaller than 11.75 meter, flooding occurs. For failure the constraint is the residual dike width, as explained in Section 3.1.3. The residual dike width is a good indicator to determine whether failure has occurred. However, there are cases where the residual width is large (so the dike still seems intact), but the residual height is relatively small (indicating that failure did occur). This can be seen in Figure 6.6. The constraints for failure are set as 12.2 for the residual height and 8.0 for the residual width. In Figure 6.6 the constraints for failure are indicated with black lines, and the constraint for flooding is indicated with a red line.

Several cases showed a residual height greater than the original height. This occurred when failure caused a single material point to float. Since this material point prevents the determination of the residual height, these cases were filtered out of the results. This reduced the number of cases to 9985.

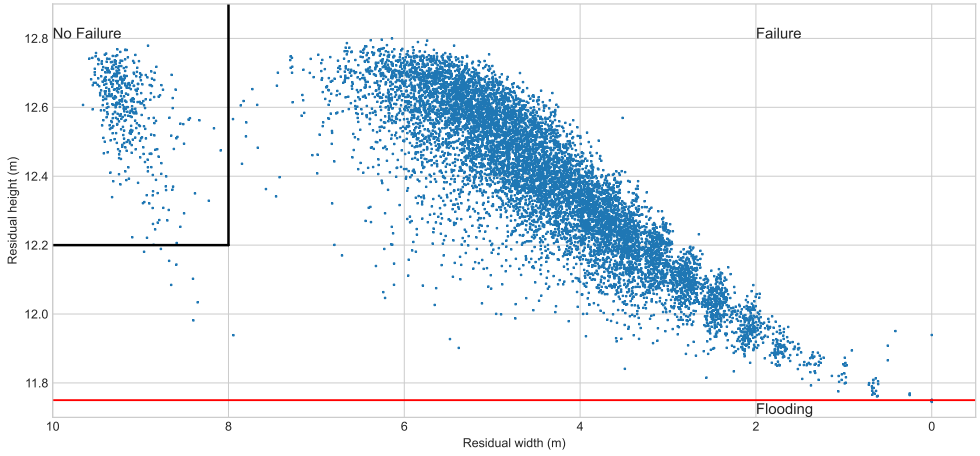

Figure 6.6: Residual width vs. residual height. *Residual Plastic Strain = 0.6*

By dividing the cases where failure or flooding happens by the total cases, the probability of flooding and failure can be determined. For the performed analysis, the results are plotted in Table 6.3 and Table 6.4.

Probability of:	Number of cases	Probability
Failure	9627	$9.64 \cdot 10^{-1}$
Flooding	64	$6.408 \cdot 10^{-3}$

Table 6.3: RMPM Monte Carlo results for 9987 cases. Residual plastic strain = 0.6

Probability of:	Number of cases	Probability
Failure	9556	$9.57 \cdot 10^{-1}$
Flooding	53	$5.308 \cdot 10^{-3}$

Table 6.4: RMPM Monte Carlo results for 9985 cases. Residual plastic strain = 0.6

In Table 6.4, it can be seen that the predicted number of cases leading to flooding by the method (52) is very close to the observed cases leading to flooding by the RMPM Monte Carlo analysis with a residual plastic strain of 0.6 (53). For the analysis with a residual plastic strain of 0.58, the number of floods is higher (64). For a residual plastic strain of 0.65 it is therefore predicted that the number of floods resulting from the RMPM Monte Carlo analysis will be lower. This is expected as the method prediction does not take into account the soil heterogeneity.

Overall the results of the analysis and the prediction by the method are very close. The method is expected to give a quick and conservative estimation for the probability of flooding of clay dikes.

6.3.2. Retrogressive Flooding

The methods in Chapter 5 gave two different flooding probabilities. One predicted flooding by retrogressive slope failure and the other method predicted flooding by a single instability. Their respective probabilities were defined as $1.369 \cdot 10^{-3}$ and $5.189 \cdot 10^{-3}$. In practice, this means that about one in every five cases that lead to flooding is caused by retrogressive slope failure, which means about ten cases from the performed analysis. To see whether this is the case, the individual cases in the RMPM Monte Carlo Analysis are analyzed.

The D-Stability calculations on the probability of flooding by retrogressive failure are given by Figures 6.7 and 6.8 and Table 6.5.

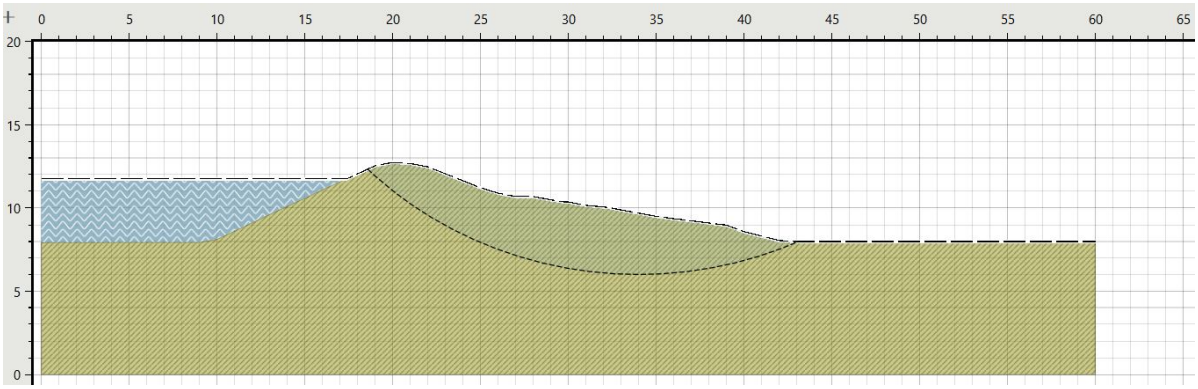

Figure 6.7: Retrogressive flooding inward dike D-Stability

Figure 6.8: Retrogressive flooding outward dike D-Stability

[-]	**Inward Dike**	**Outward Dike**	**Unit**
Probability of Failure $P(I_1)$	$1.361 \cdot 10^{-3}$	$1.369 \cdot 10^{-3}$	[−]
Reliability Index β	2.998	2.996	[−]
Design Point:	-	-	[−]
Strength Increase Exponent (m)	0.937	0.935	[−]
Shear Strength Ratio (S)	0.297	0.302	[−]
Pre-Overburden Pressure	5.278	4.826	kPa

Table 6.5: Probabilities for retrogressive failure leading to flooding

Due to the practical limitation of storage space, only the final time step of the MPM analysis could be printed. In this time step not the entire failure mechanism is shown. The cases that led to flooding by retrogressive slope failure are therefore based on two main characteristics. The first characteristic that is used to identify retrogressive failure, is the existence of multiple failure planes on the same side of the dike. This characteristic manifests itself by the presence of multiple shearing zones on the inward dike.

The second characteristic is the presence of a failure plane on the inward and outward side of the dike. As predicted by Section 5.2.2, the most likely second failure plane is situated on the outward dike although by a narrow margin.

The assumption in this analysis is that both modes of retrogressive failure are exclusive, meaning that if failure on the inward side occurs, failure on the outward side does not occur. As the probabilities of failure of the both failure mechanisms are very similar, about half of the floods by retrogressive failure are caused by sliding of the inward dike and the other half by sliding of the outward dike.

In ten of the cases where flooding occurred, at least two failures planes could be detected and retrogressive flooding was assumed. The individual cases where flooding has occurred by retrogressive slope failure are presented in Table 6.6. The cases are subdivided in a double failure plane on the inward side of the dike and on the outward side of the dike. Four cases occurred on the inward side of the dike and five cases occurred on the outward side of the dike. The cross-sections with the plotted plastic deviatoric strain invariant can be observed in Appendix B.

Case nr.	Inward or Outward?	Case nr.	Inward or Outward?
384	Inward	3025	Inward
468	Outward	6605	Outward
1356	Outward	7313	Inward
2436	Inward	7615	Outward
2891	Outward	9680	Outward

Table 6.6: Residual geometries RMPM Monte Carlo. Residual plastic strain = 0.6

The cases where the second failure plane of the dike is situated on the outside of the dike are a bit more difficult to determine. Due to some problems with the MPM model when the observed effective stress becomes very low, a distortion of material points takes place. As the model is still under development, this error still occurs in the analysis. When failure seems to occur on the outward side of the dike, the effective stress on that side becomes low and material points start to move in unexpected directions. The unexpected movement of material points can be observed in Case 468 in Figure 6.10 as opposed to the expected movement of material points in Figure 6.9.

The amount of cases where retrogressive flooding happens seems to be in line with the predictions by the method proposed to model retrogressive flooding. However, the cases where the second instability is located on the outward side of the dike cause an error in the MPM model and are therefore not questionable as results.

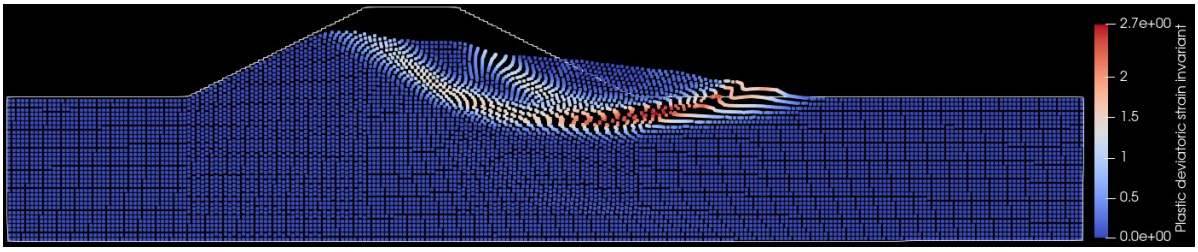

Figure 6.9: Case 2436: Retrogressive flooding inward dike

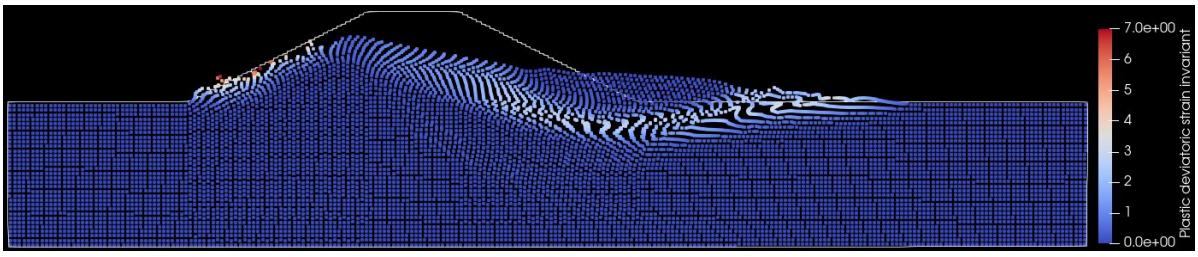

Figure 6.10: Case 468: Retrogressive flooding outward dike

6.3.3. Conclusion

The predictions made by the proposed method for flooding by a single instability seem to be in line with the results of the RMPM Monte Carlo analysis for the considered case. The probability of flooding predicted by the method of $5.308 \cdot^{-3}$coincides largely with the observed probability of flooding by the Monte Carlo analysis of $5.189 \cdot^{-3}$. The differences can be explained by the chosen value for the residual plastic strain and the implementation of heterogeneity in the RMPM model.

For the prediction of flooding by retrogressive slope failure, the results seem to be in par with the RMPM analysis as well. The MPM model experiences some material point distortion when low effective stress values occur, which manifests itself in failure of the outward dike. The expected number of floods caused by retrogressive failure coincides with the predicted number and even the expected distribution between inward and outward dike is in par with predictions. There is however a uncertainty in the cases where flooding occurred by failure of the outward dike. This aspect should be better tested when the MPM error is resolved.

7

Discussion

For many years the material point method has been a promising new technique in the field of geotechnics. A working material point method has the potential to be the most accurate method for the description of the macro-stability behavior dikes. However, the MPM model is still under construction and has some limitations that prevent it from being practically applied as the standard for dike design. The computational time of a RMPM Monte Carlo analysis is for example still a large hurdle to be taken before the model can be practically applied (Remmerswaal et al., 2018; González Acosta et al., 2020).

Despite the improvements that need to be made to the MPM model, this thesis provides a framework to practically supplement current dike design methods with the modeling of the post-failure behavior that MPM offers. The ability of the MPM model to model the post-failure behavior of dike macro-instabilities is in line with the recommendations by dike design guidelines (ENW, 2017).

However, there are limitations to the proposed method. This thesis assumed a single-layered clay dike with a water level situated at the top of the dike. The connection between D-Stability and MPM for a dike with multiple soil layers has not yet been made. The SHANSEP shear strength model was successfully implemented in (R)MPM, but has not been tested on a multi-layered dike cross-section. Moreover, due to the limited constitutive model options of MPM, a lower phreatic surface could not (yet) be included. The constraints placed on the dike case make that the proposed method is more a proof of concept that a generally applicable method. The functionality of the proposed method can however be expanded to generalize the method to be more broadly applicable.

The combination of MPM and D-Stability, within the applied constraints, shows promising results, as the probability of flooding and failure behaviour corresponds largely with results from RMPM. However, a note has to be made that RMPM is still under development and that the analysis results should be viewed in that light. It is possible that some errors have remained undetected by the large number of simulations that were ran. Although, the results of RMPM showed some irregularities for some cases, the overall outcome forms an indication of the potential of combining MPM and D-Stability, especially for (but not limited to) the specific application tested here.

The main advantage of the proposed method over the RMPM Monte Carlo analysis, is the time duration. Where a RMPM Monte Carlo analysis can take up to several days to compute, and even several hours on a grid computing system, the proposed method can be conducted in about two hours on a desktop, depending on the required number of MPM simulations. The disadvantage is that the method has no room to incorporate the heterogeneity of the soil. The result of the method should therefore be still a conservative estimate of the actual dike situation.

The user-friendliness of the proposed method is also a hurdle that needs to be taken. Several Python scripts are required to perform the method and they are preferably to be understood by the user. It may take some time to become familiar with the use of the scripts and the required input of the scripts. Although relatively quick, the proposed method is generally difficult in use and a deeper understanding of the different methods used is required.

The estimation of the flooding probability by retrogressive failure is discussed by Van der Krogt et al. (2019) as a potentially critical flooding mechanism. Although flooding by retrogressive failure could be the potentially most critical failure mechanism, the cases in this thesis had flooding by a single slip surface as most critical failure mechanism, roughly five times more frequent than retrogressive failures. Flooding by

retrogressive slope failure may be the critical flooding mechanism for some dike cases, but that was not the case for the considered (simplified) case study.

Overall a bridge was created between D-Stability and the MPM model that has the potential to gain more information on the post-failure behavior for D-Stability calculations. Although this thesis used some constraints in the connection between both methods, the potential is there to increase the integration of both methods. This is especially useful when considering flooding by retrogressive slope failure. However, retrogressive slope failure is not necessarily the most critical flooding mechanism for macro-instability, but this is difficult to determine up front.

8

Conclusion

Current probabilistic methods for the determination of the macro-stability of dikes have some disadvantages. For D-Stability the a probabilistic analysis is quickly performed but the result does not give much information on the post-failure behavior. The Material Point Method is ideal for determining the post-failure behavior, but has as disadvantage that a (probabilistic) calculation takes very long. It is therefore for both methods impractical to quickly determine the probability of flooding.

By linking D-Stability and the MPM model by implementing the SHANSEP shear strength model in the MPM model, the advantages of both D-Stability and MPM have been exploited while the disadvantages of both methods were mitigated. By transferring between D-Stability and MPM the probability of flooding can be estimated relatively quickly.

By means of a cases study it was shown that the proposed method is practical in assessing two types of flooding: by retrogressive slope failure and by failure via a single instability. Three methods were proposed to compute the probability of flooding conditional to the water level. Method 1 determines the probability of retrogressive flooding for different water levels. Method 2 determines the probability of flooding for predetermined critical water levels. Method 3 determines the probability of flooding by a single instability for multiple water levels. In the case presented, flooding by a single instability appeared to be most critical, occurring roughly five times more frequently than a single instability.

The SHANSEP shear strength model was implemented into RMPM so a random Monte Carlo analysis could be made. The RMPM results corresponded to the results predicted by the proposed method. The proposed is thus successful in predicting the probability of flooding and also the failure mechanisms leading to flooding.

The method was able to estimate the probability of flooding. However, there are some disadvantages to the model. Although the computation time of the method is shorter than the computation time of RMPM, it still takes around three hours to perform a full analysis. Besides the longer computation time, the method is difficult to put into practice and requires a thorough understanding of the different method components.

There is overall a lot of potential to combine D-Stability and the Material Point Method. The proposed methods can be practically applied to assess the post-failure behavior of the most likely instability, estimate the probability of flooding by retrogressive slope failure and estimate the probability of flooding by a single instability. These options can help to more efficiently design waterworks by including the impact of failure. They may also be useful for the estimation of the consequence of failure in other geotechnical applications.

9

Recommendations

The method proposed in this thesis has proven to be effective with the limitations applied to it. The method is a viable option for dike assessment in the future, after some limitations have been removed. These limitations prevent the method from being generally applicable at this stage. However, once these limitations have been reduced, the combination of D-stability and MPM should be considered in practice.

One of the limitations of the method is that it currently only works for a single soil layer. It is recommended that the transfer of multiple soil layers between D-Stability and MPM is added. A better option would be a complete integration of MPM and D-stability, i.e. LEM, in the same commercial software. The input parameters of D-Stability can then directly serve as input for MPM, the geometry could be more easily updated, and the processing of results would simplify. This would reduce the computation time and improve the user-friendliness.

As MPM is still under development only the Von-Mises constitutive model for clay was considered in this case. When more soil models are incorporated into MPM the connection with D-Stability should be reassessed per constitutive model. The incorporation of more soil models would increase the general applicability of the proposed method.

An important factor in the behavior of the dike is the elasticity. For this thesis a single elasticity value was used for the entire dike cross-section. In reality the elasticity is stress-dependent. It is therefore recommended to add a stress-dependent elasticity term in MPM. To do so, the code that calculates the stress dependent undrained shear strength on the material points can be adjusted to give each material point its own elasticity value.

To reduce the computation time a mesh with larger elements would be more efficient. It could be investigated whether a relationship exists between the mesh size and the strength parameters. By adjusting the strength parameters to the mesh size, potentially a smaller mesh could be used, increasing the computational speed of the method.

The final recommendation that would improve the method is the implementation of different failure mechanisms. This thesis focused solely on the dike macro-stability as failure mechanism, however other failure mechanisms that can lead to flooding exist as well. When MPM is further developed and is able to incorporate pore water pressures, the elements of uplift and piping for example can be added, potentially removing the need to split failure probability over multiple mechanisms.

To make the method more generally applicable, it is recommended that these limitations will be gradually lifted in further research.

Bibliography

[1] S.M. Andersen and L.V. Andersen. Modeling of landslides with the material point method. *Computational Geosciences*, 14:137–147, 2010. doi: https://doi.org/10.1007/s10596-009-9137-y.

[2] Tamer Elkateb, Rick Chalaturnyk, and P.K. Robertson. An overview of soil heterogeneity: Quantification and implications on geotechnical field problems. *Canadian Geotechnical Journal*, 40:1–15, 2003. doi: 10.1139/t02-090.

[3] ENW. Fundamentals of flood protection. *Ministerie van Infrastructuur en Milieu*, 2017.

[4] Pooyan Ghasemi, Mario Martinelli, Sabatino Cuomo, and Michele Calvello. Mpm modelling of static liquefaction in reduced-scale slope. *Conference: Numerical Methods in Geotechnical Engineering IX*, 1: 555–581, 2018. doi: 10.1007/s00466-019-01783-3.

[5] José León González Acosta, Philip J. Vardon, Guido Remmerswaal, and Michael A. Hicks. An investigation of stress inaccuracies and proposed solution in the material point method. *Computational Mechanics*, 65:555–581, 2020. doi: 10.1007/s00466-019-01783-3.

[6] E.J. Gumbel. The return period of flood flows. *Annals of Mathematical Statistics*, 12:163–190, 1941. doi: 10.1214/aoms/1177731747.

[7] L. Jing. A review of techniques, advances and outstanding issues in numerical modelling for rock mechanics and rock engineering. *International Journal of Rock Mechanics and Mining Sciences*, 40:283–353, 2003. doi: https://doi.org/10.1016/S1365-1609(03)00013-3.

[8] S.N. Jonkman, H.M.G.M. Steenbergen, O Morales-Nápoles, A.C.W.M. Vrouwenvelder, and J.K. Vrijling. Probabilistic design: Risk and reliability analysis in civil engineering. *TU Delft*, 2016.

[9] M. Kok, R.B. Jongejan, M. Nieuwjaar, and I. Tánczos. Grondslagen voor hoogwaterbescherming. *Expertise Netwerk Waterveiligheid*, 2016.

[10] Mario Martinelli, Alexander Rohe, and Soga Kenichi. Modeling dike failure using the material point method. *Procedia Engineering*, 175:341–348, 2017. doi: 10.1016/j.proeng.2017.01.042.

[11] Guido Remmerswaal, M. A. Hicks, and P. J. Vardon. Ultimate limit state assessment of dyke reliability using the random material point method. *Book of extended abstracts 4th international symposium on computational geomechanics*, pages 89–90, 2018. doi: http://resolver.tudelft.nl/uuid:731df946-b05b-44f6-a2c1-e7c20f559619.

[12] Timo Schweckendiek, Mark Van der Krogt, Ana. Teixeira, Wim Kanning, Rob Brinkman, and Katerina Rippi. Reliability updating with survival information for dike slope stability using fragility curves. *American Society of Civil Engineers*, 2017. doi: 10.1061/9780784480700.047.

[13] H.M.G.M. Steenbergen, B.L. Lassing, A.C.W.M. Vrouwenvelder, and P.H. Waarts. Reliability analysis of flood defence systems. *Heron*, 49, 2004.

[14] Technical Advisory Committee on Water Defenses TAW. Fundamentals on water defences. *http://www.tawinfo.nl*, 1998.

[15] Takashi Tsuchida and A.M.R.G. Athapaththu. Practical slip circle method of slices for calculation of bearing capacity factors. *Soils and Foundations*, 55:484, 2015. doi: https://doi.org/10.1016/j.sandf.2014.11.008.

[16] USACE. Engineering and design: Settlement analysis, 1990. URL `https://www.publications.usace.army.mil/Portals/76/Publications/EngineerManuals/EM_1110-1-1904.pdf`.

[17] USACE. Engineering and design: Slope stability, 2003. URL https://www.publications.usace.army.mil/Portals/76/Publications/EngineerManuals/EM_1110-2-1902.pdf.

[18] Bram van den Eijnden. Advanced fem - part ii. *CIE4366: Numerical Modelling in Geo-Engineering*, 2018.

[19] Mark Van der Krogt, Timo Schweckendiek, and Matthijs Kok. Do all dike instabilities cause flooding? *13th International Conference on Applications of Statistics and Probability in Civil Engineering (ICASP13)*, 2019. doi: I10.22725/ICASP13.461.

[20] R. Van der Meij. D-stability user manual. *Deltares*, 2020.

[21] Mick Van Montfoort. Safety assessment method for macro-stability of dikes with high foreshores. *TU Delft*, 2018.

[22] Phil Vardon. The inner workings of fem. *CIE4366: Numerical Modelling in Geo-Engineering*, 2018.

[23] Bin Wang. *Slope failure analysis using the material point method*. PhD thesis, Delft University of Technology, 2017.

[24] Bin Wang, Philip J. Vardon, Michael A. Hicks, and Zhen Chen. Development of an implicit material point method for geotechnical applications. *Computers and Geotechnics*, 71:159–167, 2015. doi: https://doi.org/10.1016/j.compgeo.2015.08.008.

A

Appendix A - Sensitivity Analysis Results

This Appendix shows the calculations performed for the sensitivity analysis.

Input Parameter	**Dike 1**	**Dike 2**	**Unit**
Unit Weight (γ)	18	18	kN/m^3
Shear Strength Ratio (S)	0.36	0.36	[-]
Strength Increase Exponent (m)	0.98	0.98	[-]
Pre-Overburden Pressure	15.6	16	kPa
Water Level Left	10	10	m
Factor of Safety	1.0	1.011	[-]

Table A.1: D-Stability Input Parameters Factor of Safety equals 1.0

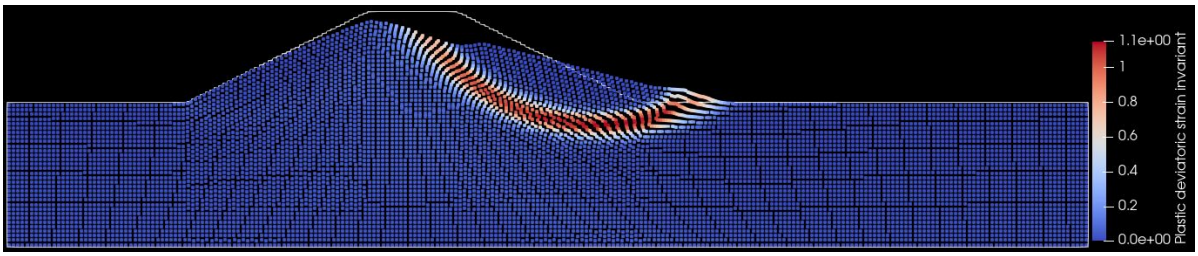

Figure A.1: Dike 1: failure occurs. $Hs = 9.5$

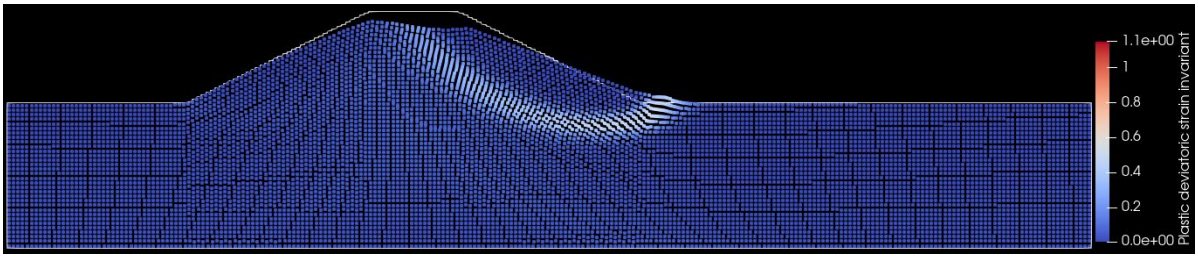

Figure A.2: Dike 2: failure does not occur. $H_s = 9.5$

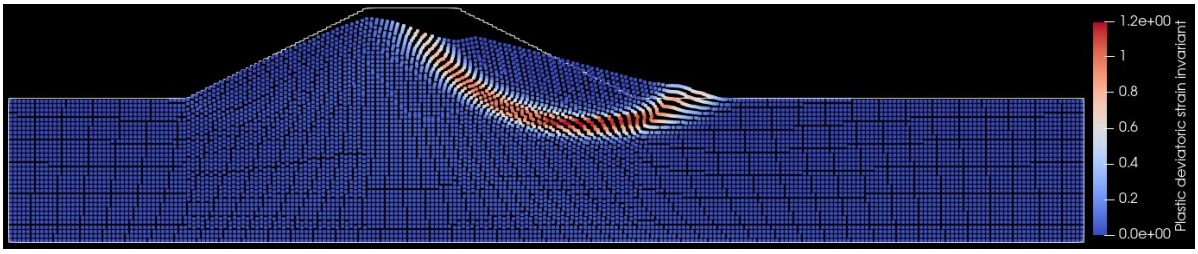

Figure A.3: Dike 1: failure occurs. $\epsilon_p^r = 0.65$

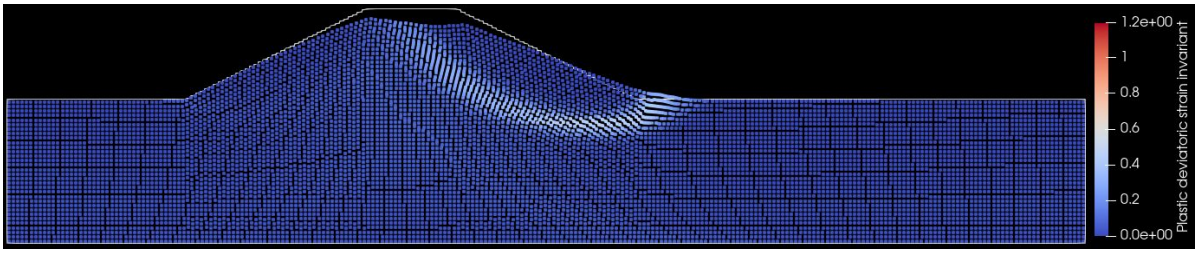

Figure A.4: Dike 2: failure does not occur. $\epsilon_p^r = 0.65$

B

Appendix B - RMPM Retrogressive Flooding Residual Geometries

This appendix shows the cases of the RMPM Monte Carlo analysis of Chapter 6 where flooding by retrogressive failure occurred. The cases where flooding occurs by retrogressive flooding are given in Tables B.1 and B.2. In Table B.3 it is specified whether failure occurs on the inward or the outward side of the dike.

Case nr.	Retrogressive?	Case nr.	Retrogressive?	Case nr.	Retrogressive?	Case nr.	Retrogressive?
384	Yes	2089	No	2891	Yes	5037	No
468	Yes	2287	No	2927	No	5717	No
494	No	2436	Yes	3025	Yes	5804	No
604	No	2490	No	3056	No	5859	No
905	No	2594	No	3321	No	6203	No
1228	No	2597	No	3473	No	6345	No?
1356	Yes	2710	No	3866	No	6469	No
1636	No	2755	No	3971	No	6479	No
1796	No	2779	No	4540	No	6513	No
2010	No	2872	No	4672	No?	6605	Yes

Table B.1: Residual geometries RMPM Monte Carlo. Residual Plastic Strain = 0.6

Case nr.	Retrogressive?	Case nr.	Retrogressive?
7182	No	8354	No
7249	No	8467	No
7313	Yes	8491	No
7479	No?	8987	No
7615	Yes	9680	Yes
7965	No	9867	No
8090	No		

Table B.2: Residual geometries RMPM Monte Carlo. Residual plastic strain = 0.6

Case nr.	Inward or Outward?	Case nr.	Inward or Outward?
384	Inward	3025	Inward
468	Outward	6605	Outward
1356	Outward	7313	Inward
2436	Inward	7615	Outward
2891	Outward	9680	Outward

Table B.3: Residual geometries RMPM Monte Carlo. Residual Plastic Strain = 0.6

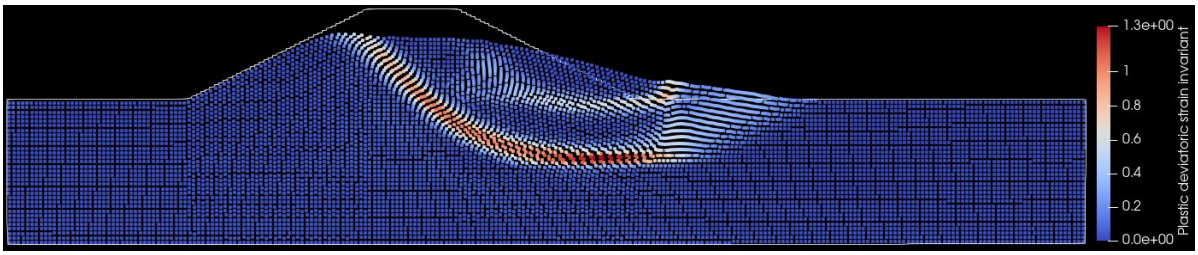

Figure B.1: Case 384: Retrogressive flooding inward dike

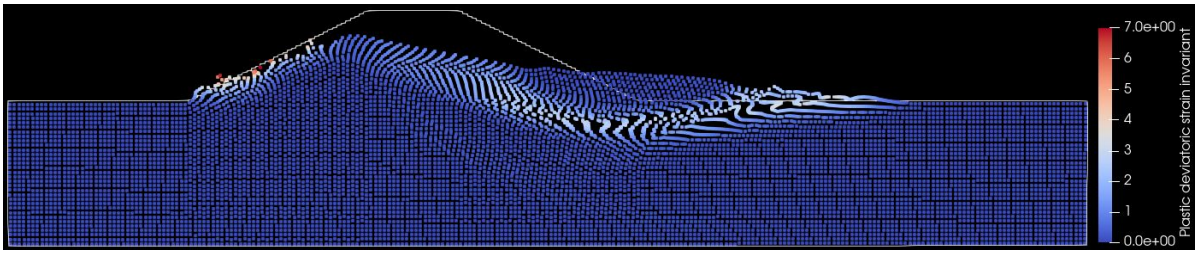

Figure B.2: Case 468: Retrogressive flooding outward dike

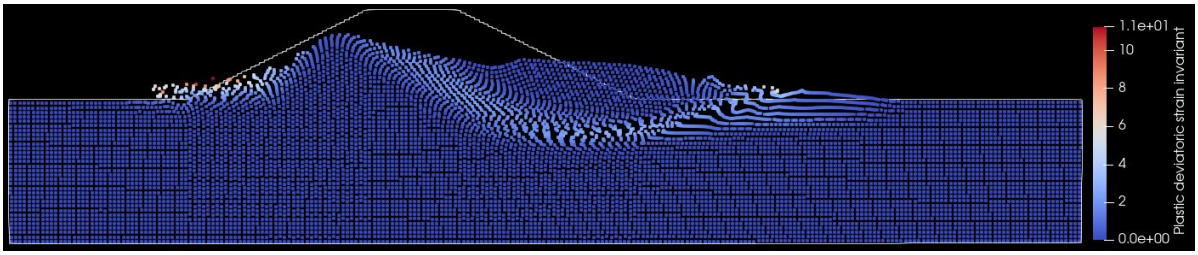

Figure B.3: Case 1356: Retrogressive flooding outward dike

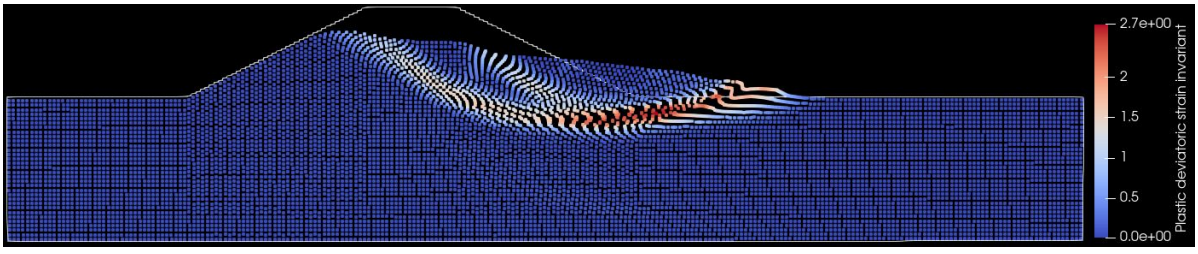

Figure B.4: Case 2436: Retrogressive flooding inward dike

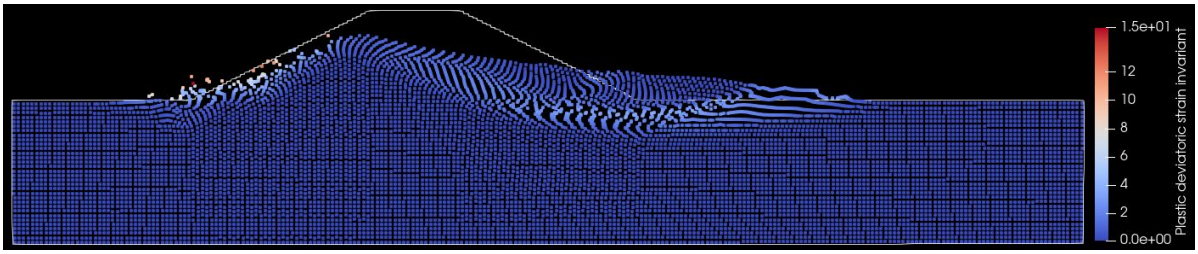

Figure B.5: Case 2891: Retrogressive flooding outward dike

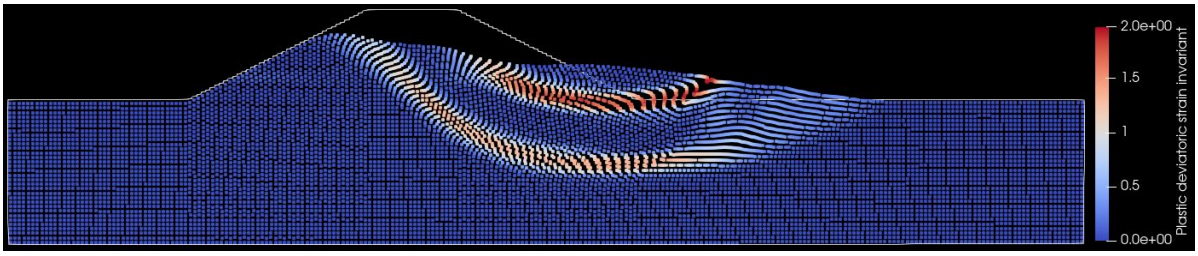

Figure B.6: Case 3025: Retrogressive flooding inward dike

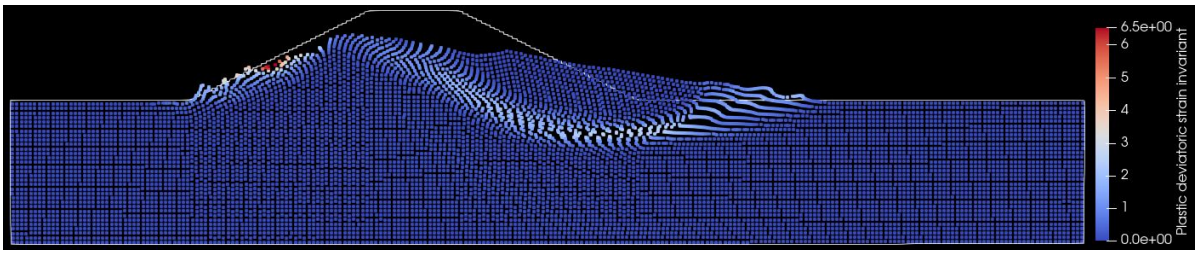

Figure B.7: Case 6605: Retrogressive flooding outward dike

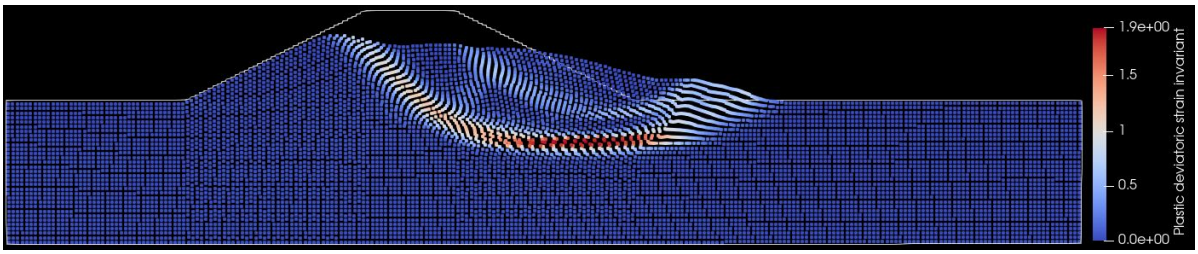

Figure B.8: Case 7313: Retrogressive flooding inward dike

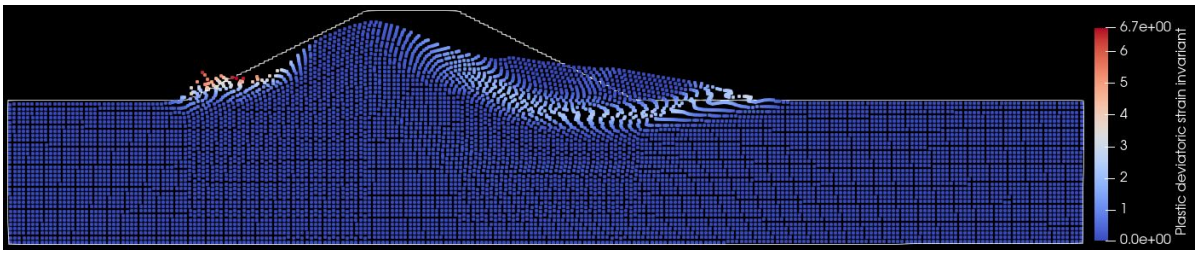

Figure B.9: Case 7615: Retrogressive flooding outward dike

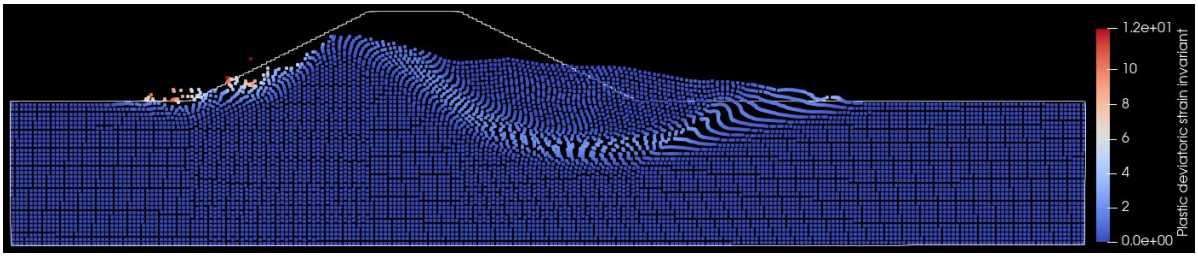

Figure B.10: Case 9680: Retrogressive flooding outward dike